

TOPICAL REVIEW • OPEN ACCESS

## Non-thermal plasma catalysis for CO<sub>2</sub> conversion and catalyst design for the process

To cite this article: Shanshan Xu *et al* 2021 *J. Phys. D: Appl. Phys.* **54** 233001

View the [article online](#) for updates and enhancements.

You may also like

- [An intermediate state of T7 RNA polymerase provides another pathway of nucleotide selection](#)  
Zhan-Feng Wang, , Yu-Ru Liu et al.
- [Ammonia synthesis by nonthermal plasma catalysis: a review on recent research progress](#)  
Yuxin Zhang, Jiangqi Niu, Shaowei Chen et al.
- [Assessment of an NTP service calibration over a Local Area Network](#)  
Carmen Vélez, Javier Díaz, Alfonso Osuna et al.



**UNITED THROUGH SCIENCE & TECHNOLOGY**

 The Electrochemical Society  
Advancing solid state & electrochemical science & technology

**248th  
ECS Meeting**  
Chicago, IL  
October 12-16, 2025  
*Hilton Chicago*

**Science +  
Technology +  
YOU!**

**SUBMIT  
ABSTRACTS by  
March 28, 2025**

**SUBMIT NOW**

## Topical Review

# Non-thermal plasma catalysis for CO<sub>2</sub> conversion and catalyst design for the process

Shanshan Xu<sup>1</sup>, Huanhao Chen<sup>2,\*</sup>, Christopher Hardacre<sup>1,\*</sup> and Xiaolei Fan<sup>1,\*</sup> 

<sup>1</sup> Department of Chemical Engineering and Analytical Science, School of Engineering, The University of Manchester, Manchester M13 9PL, United Kingdom

<sup>2</sup> State Key Laboratory of Materials-Oriented Chemical Engineering, College of Chemical Engineering, Nanjing Tech University, Nanjing 210009, People's Republic of China

E-mail: [h.chen@njtech.edu.cn](mailto:h.chen@njtech.edu.cn), [c.hardacre@manchester.ac.uk](mailto:c.hardacre@manchester.ac.uk) and [xiaolei.fan@manchester.ac.uk](mailto:xiaolei.fan@manchester.ac.uk)

Received 30 November 2020, revised 16 February 2021

Accepted for publication 25 February 2021

Published 17 March 2021



## Abstract

Catalytic conversion of CO<sub>2</sub> to renewable chemicals and fuels is a promising approach to mitigate issues associated with climate change and energy supply deficiency. Hybrid non-thermal plasma (NTP) and catalysis systems, that is, NTP catalysis systems, enable the activation of stable CO<sub>2</sub> molecules under relatively mild conditions in comparison with conventional thermal catalysis, and are promising for the energy-efficient conversion of CO<sub>2</sub>. This review presents the state-of-the-art development of NTP catalysis of CO<sub>2</sub> conversion, including CO<sub>2</sub> splitting and CO<sub>2</sub> hydrogenation and reforming, with the focus on mechanistic insights developed for catalytic CO<sub>2</sub> conversion. Additionally, the role of intrinsic catalyst composition and structure in determining the selectivity of CO<sub>2</sub> conversion under NTP conditions is also discussed in light of the need for rational design of catalysts for NTP catalysis. Finally, a perspective on future challenges and opportunities in the development of next-generation catalysts for NTP catalysis and the advanced hybrid NTP catalysis process for practical industrial applications are discussed.

Keywords: non-thermal plasma (NTP), heterogeneous catalysis, CO<sub>2</sub> conversion, mechanism

(Some figures may appear in colour only in the online journal)

## 1. Introduction

Carbon dioxide (CO<sub>2</sub>) emissions are the main contributor to global warming and climate change. The catalytic conversion of CO<sub>2</sub> to renewable and valuable chemicals and fuels is a

promising method to mitigate these issues and contribute to the development of a sustainable low-carbon economy [1, 2]. CO<sub>2</sub> conversion is challenging due to the high thermodynamic stability and ionisation potential of the linear CO<sub>2</sub> molecule (bond enthalpy = +805 kJ mol<sup>-1</sup>). Typically, high temperatures and/or pressures are required to activate CO<sub>2</sub> under conventional thermal conditions, which are associated with high energy demand and cause catalyst deactivation [3].

Non-thermal plasmas (NTPs), with a mean electron energy of 1–10 eV, could activate and dissociate ground-state gas molecules to generate various active species including vibrationally excited molecules, atoms, ions and radicals, allowing

\* Authors to whom any correspondence should be addressed.



Original content from this work may be used under the terms of the [Creative Commons Attribution 4.0 licence](https://creativecommons.org/licenses/by/4.0/). Any further distribution of this work must maintain attribution to the author(s) and the title of the work, journal citation and DOI.

reactions to occur at relatively mild bulk temperatures and atmospheric pressure [4–6]. Accordingly, NTP catalysis is capable of promoting many energy-intensive and kinetically and/or thermodynamically limited heterogeneous catalytic reactions such as CO<sub>2</sub> hydrogenation [7, 8], the water-gas shift reaction [9, 10], hydrocarbon reformation [11–13], pollutant decomposition [14] and ammonia synthesis [15, 16].

Although NTPs alone can break the chemical bond of the CO<sub>2</sub> molecule without a catalyst, selectivity towards desired products (e.g. CH<sub>4</sub>, hydrocarbons and oxygenates) is poor due to the unselective collisions between the active species [17]. Thus the integration of plasma discharge with catalysts (known as NTP catalysis) is proposed for enhancing CO<sub>2</sub> conversion and regulating the product distribution [18]. Under NTP conditions, catalysts enable additional reaction pathways via surface reactions which increase the product selectivity. The physical and chemical properties of the catalysts play a key role in the NTP catalysis because their presence can affect the electric field intensity, as well as lead to surface discharges, thereby enhancing electron energy distribution and affecting interactions between the plasma and catalysts [19, 20]. Additionally, plasma-induced short-lived reactive species deactivate quickly via recombination and/or quenching in the gas-phase before accessing the catalyst surface and participating in surface reactions [21, 22]. Thus, the location of the active sites in the catalyst is also important regarding the performance of the NTP catalysis.

Designing and developing efficient and cost-effective catalysts for NTP catalysis requires a thorough understanding of the mechanisms of NTP catalysis regarding the transport of reactive species, surface reaction chemistry and plasma discharge properties. However, these studies are challenging due to the complex nature of NTP catalysis [23]. Accordingly, advanced *in situ* techniques [22, 24] and modelling methods [16, 17, 25] are needed to enable a mechanistic understanding of NTP catalysis for the rational design of bespoke catalysts to be used in NTP catalysis, as well as the optimisation of NTP catalytic systems with respect to the reaction rate, selectivity and energy efficiency for CO<sub>2</sub> conversion.

In this review, state of the art of NTP catalytic systems for CO<sub>2</sub> conversion including CO<sub>2</sub> splitting, CO<sub>2</sub> hydrogenation and reforming are presented first. Then, the role of the catalyst structure in determining the CO<sub>2</sub> conversion under thermal and NTP conditions are compared, which can shed light on a strategy for the rational design of bespoke catalysts for advanced NTP catalysis. Finally, recent progress on a mechanistic understanding of NTP catalysis via *in situ* characterisation and modelling studies is discussed.

## 2. NTP catalysis for CO<sub>2</sub> conversion

NTP catalysis is effective in activating and converting CO<sub>2</sub> into various chemicals and fuels such as CO, methane (CH<sub>4</sub>), hydrocarbons and oxygenates under mild conditions, as illustrated in figure 1. Specifically, a dielectric barrier discharge (DBD) reactor with two coaxial electrodes is widely employed under NTP conditions for CO<sub>2</sub> conversion in the presence of

catalysts. The simple configuration of the DBD reactor and ambient operating conditions (i.e. at atmospheric pressure and low temperatures) is attractive for possible industrial exploitation [17, 26]. However, fundamental investigations into the mechanisms of CO<sub>2</sub> conversion are still needed due to the coexistence of gas-phase and surface reactions and complex plasma–catalyst interactions. Therefore, the following discussion will outline recent progress in NTP catalytic CO<sub>2</sub> conversion in DBD reactors and relevant exploration of the reaction mechanism/pathways underlying CO<sub>2</sub> conversion.

### 2.1. Definition of key performance indicators for assessing NTP catalytic CO<sub>2</sub> conversion

To compare the various plasma-catalytic systems for CO<sub>2</sub> conversion, a summary of the key performance indicators, including conversion ( $\chi$ ), selectivity, yield, specific energy input (SEI) and energy efficiency ( $\eta$ ), are introduced in this section.

The standard expression for ‘conversion’ used in the literature is provided in equation (2.1) for the converted reactants (e.g. CO<sub>2</sub> and CH<sub>4</sub>), and the selectivity is defined as the amount of the produced target product divided by the converted reactant (equation (2.2)). The yield of the desired product can be calculated by multiplying the conversion by the selectivity of the desired product (equation (2.3)):

$$\chi_{\text{reactant}_i} = \frac{\dot{n}_{\text{reactant}_i,\text{in}} - \dot{n}_{\text{reactant}_i,\text{out}}}{\dot{n}_{\text{reactant}_i,\text{in}}}, \quad (2.1)$$

$$S_{\text{product}_i} = \frac{\dot{n}_{\text{product}_i,\text{out}}}{\dot{n}_{\text{reactant}_i,\text{in}} - \dot{n}_{\text{reactant}_i,\text{out}}}, \quad (2.2)$$

$$Y_{\text{product}_i} = \chi_{\text{reactant}_i} \times S_{\text{product}_i}, \quad (2.3)$$

where  $\dot{n}$  stands for the molar flow rate of the reactant or desired product.

The SEI (expressed as J cm<sup>-3</sup> or kJ l<sup>-1</sup>) is defined as the power (used for generation of the plasma discharge) divided by the gas flow rate, which is the determining factor in the conversion and energy efficiency in plasma systems:

$$\text{SEI (J cm}^{-3}\text{)} = \frac{\text{Power (W)}}{\text{Flowrate (ml s}^{-1}\text{)}}. \quad (2.4)$$

The energy efficiency ( $\eta$ ) depends on the plasma process under study. It was introduced to assess the efficiency of the plasma process (for the conversion of CO<sub>2</sub>) as compared with the standard reaction enthalpy:

$$\eta = \frac{\chi_{\text{Total}} \times \Delta H_{298\text{K}}^{\circ}}{\text{SEI}}, \quad (2.5)$$

where  $\chi_{\text{Total}}$  is the total conversion of the process and  $\Delta H_{298\text{K}}^{\circ}$  is the standard enthalpy.

### 2.2. CO<sub>2</sub> splitting

Plasma-activated CO<sub>2</sub> splitting into CO and O<sub>2</sub> has been intensively investigated since CO is an important chemical

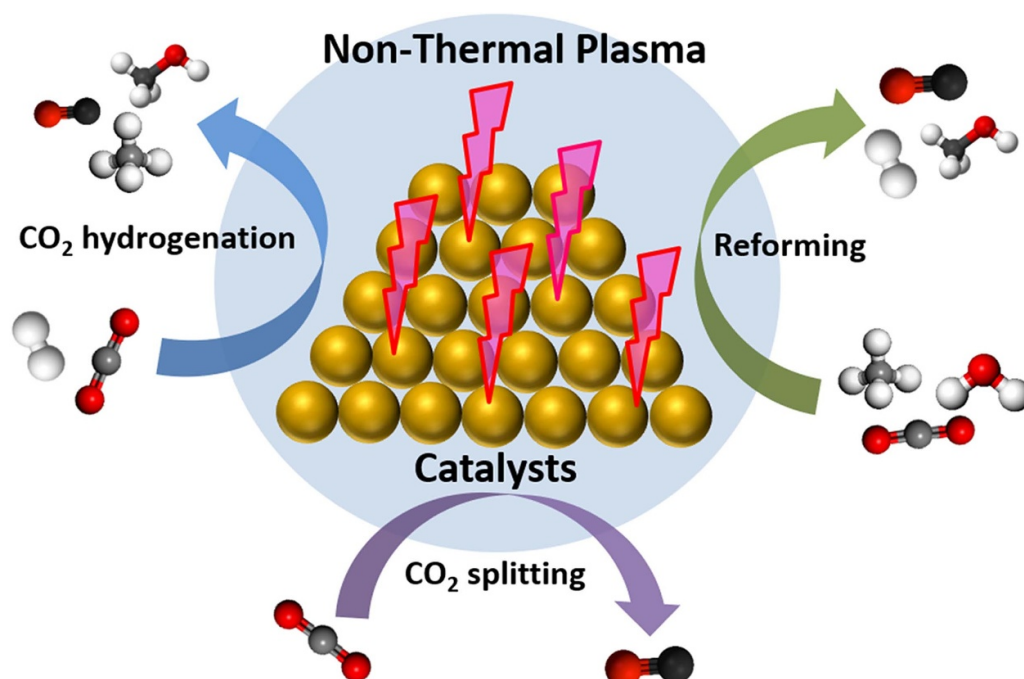


Figure 1. NTP-activated heterogeneous catalysis for CO<sub>2</sub> conversion.

feedstock for synthetic fuels through the Fischer–Tropsch and methanol synthesis processes [27, 28]. Typically, CO<sub>2</sub> splitting can be activated only under NTP conditions (without a catalyst), and CO<sub>2</sub> conversion can be improved by increasing the SEI due to the increased average electron density [29, 30]. CO<sub>2</sub> splitting under NTP conditions is dominated by electron-impact dissociation (forming CO and O atoms and ions), the ionisation process (forming CO<sub>2</sub><sup>+</sup> ions) and electron dissociative attachment (forming CO and O<sup>-</sup> ions). However, a fraction of the ions from these processes (e.g. CO and O) can recombine to CO<sub>2</sub> in the gas phase. Therefore, the plasma-only system is intrinsically energy intensive, its highest achievable CO<sub>2</sub> conversion rate is ~30% and it has a relatively low energy efficiency of 5%–10% [17, 31]. The addition of inert gases (e.g. helium and argon) into this system can also promote CO<sub>2</sub> conversion but the energy efficiency decreases due to the significant amount of energy used in the excitation of He or Ar atoms [32, 33]. CO<sub>2</sub> conversion and energy efficiency can be improved using packing materials in DBD reactors, such as glass beads [34], quartz [35], Al<sub>2</sub>O<sub>3</sub> [35–37], BaTiO<sub>3</sub> [38, 39], SiO<sub>2</sub> [36] and ZrO<sub>2</sub> [40]. The packing materials affect the physical characteristics of the plasma discharge, which enhance the electric field and enable the formation of surface discharges and micro-discharges, thus promoting gas-phase CO<sub>2</sub> dissociation. However, these systems cannot be classified as NTP catalysis. By incorporating a catalyst, the CO<sub>2</sub> conversion and energy efficiency in CO<sub>2</sub> splitting under plasma conditions can be improved. For example, using a Ni/γ-Al<sub>2</sub>O<sub>3</sub> catalyst within a DBD reactor, comparably high CO<sub>2</sub> conversion (~26.3%) and energy efficiency (~4.1%) were achieved as compared with the reference NTP system with BaTiO<sub>3</sub> packing [41]. It was found that, in addition to the electron-impact dissociation of CO<sub>2</sub> in the gas

phase, the ground state and excited states of CO<sub>2</sub> can adsorb on the Ni surface and subsequently dissociate into CO and O with the assistance of energetic electrons, explaining the improved system performance. However, as compared with the performance data presented in the current literature, NTP catalytic systems for selective CO<sub>2</sub> splitting still require further development and improvement.

### 2.3. CO<sub>2</sub> hydrogenation

CO<sub>2</sub> hydrogenation with molecular H<sub>2</sub> can produce a range of chemicals, including CO, CH<sub>4</sub>, hydrocarbons and oxygenates (methanol, dimethyl ether, ethanol, etc). Conversion of CO<sub>2</sub> to CO via the reverse water–gas shift (RWGS) reaction and CH<sub>4</sub> via CO<sub>2</sub> methanation (the Sabatier reaction) under NTP conditions has been investigated [7, 42]. Zhu *et al* [43] studied the effect of a plasma on RWGS over an Au/CeO<sub>2</sub> catalyst. Therein, the plasma enabled a CO<sub>2</sub> conversion rate of ~25.5%, which was higher than the thermodynamic equilibrium value of ~22% at 400 °C. As compared with conventional thermal catalysis, NTP catalysis can create high concentrations of reactive species, which improves the CO<sub>2</sub> methanation rate and CH<sub>4</sub> yield at low operating temperatures [44]. For example, Biset-Peiró *et al* [45] compared catalytic CO<sub>2</sub> methanation over a Ni–CeO<sub>2</sub>/Al<sub>2</sub>O<sub>3</sub> catalyst under thermal and NTP conditions. A CO<sub>2</sub> conversion of 70% and CH<sub>4</sub> yield of 96% was achieved under NTP conditions (at ~150 °C), whereas under thermal conditions, a temperature in excess of 350 °C was required to achieve a similar performance. Similar results have been reported by other studies as well [46]. In NTP catalysis, highly reactive species contribute to CO<sub>2</sub> methanation; for example, vibrationally excited CO<sub>2</sub> can adsorb on the catalyst surface to lower the energy barrier as

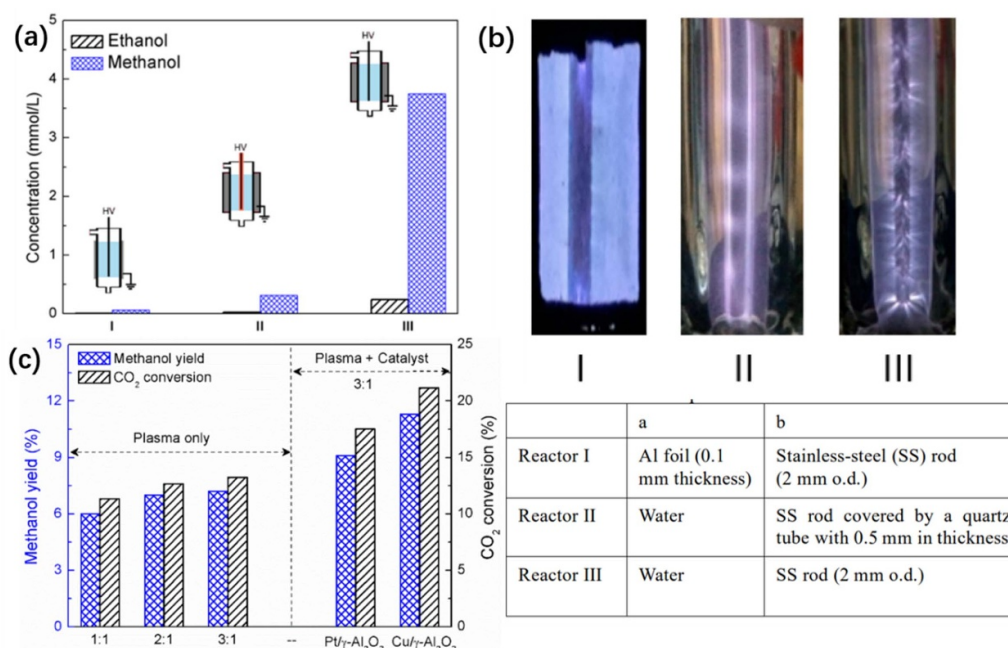


**Figure 2.** (a) The influence of DBD reactor configurations on  $\text{CO}_2$  hydrogenation to methanol under NTP conditions. (b) Images of  $\text{H}_2/\text{CO}_2$  discharge generated in different DBD reactors. (c) Effect of  $\text{H}_2/\text{CO}_2$  molar ratio and catalysts on reaction performance. Reprinted with permission from [52]. Copyright (2018) American Chemical Society.

compared with the ground-state  $\text{CO}_2$  and facilitate the formation of reactive intermediates on the catalyst surface [19]. Conversely, in thermal catalysis,  $\text{CO}_2$  needs to be adsorbed and activated by the catalyst surface before surface reactions can take place, demanding high temperatures [47]. Additionally, the NTP-induced excited states of other reactive species such as CO, OH and CH radicals in the gas phase can also readily interact with the catalyst to promote relevant surface reactions [24, 48].

In addition to CO and  $\text{CH}_4$ , hydrocarbons and oxygenates, especially methanol, are valuable fuel substitutes and key feedstocks for a wide range of products such as polymers, solvents, and drugs. Catalytic  $\text{CO}_2$  hydrogenation into hydrocarbons and methanol under thermal conditions is usually conducted at high temperatures and pressures [49]; thus the integration of plasma with catalysts to enable these conversions efficiently under mild conditions is important. Lan *et al* [50] reported that Co/ZSM-5 catalysts promoted hydrocarbon formation with a  $\text{C}_2\text{--C}_4$  selectivity of 13.7% at 45.0%  $\text{CO}_2$  conversion under NTP.  $\text{CO}_2$  hydrogenation into methanol under NTP conditions was explored by Eliasson *et al* [51]. Therein, the methanol yield/selectivity was enhanced by a factor of >10 by coupling NTP with a commercial CuO/ZnO/ $\text{Al}_2\text{O}_3$  catalyst at  $\sim 100^\circ\text{C}$  compared with the results under NTP-only conditions. Recently, Wang *et al* [52] presented a significant improvement in  $\text{CO}_2$  hydrogenation to methanol (i.e. 14%  $\text{CO}_2$  conversion and 53.7% methanol selectivity) using a specially designed DBD reactor with a water-cooled electrode (as shown in figures 2(a) and (b)). This setup efficiently removed the heat generated by Joule heating and the reaction exothermicity to maintain the NTP system at  $\sim 30^\circ\text{C}$ . In this work, the catalytic performance of the Pt/ $\gamma\text{-Al}_2\text{O}_3$  and Cu/ $\gamma\text{-Al}_2\text{O}_3$  catalysts was investigated,

as shown in figure 2(c), in which Cu/ $\gamma\text{-Al}_2\text{O}_3$  presented a relatively good catalytic performance (i.e. 21.2%  $\text{CO}_2$  conversion and 11.3% methanol yield), showing that both the plasma reactor and the catalyst design can affect catalysis under NTP conditions. However, it is obvious that practical applications of  $\text{CO}_2$  hydrogenation to methanol are still some way off due to the relatively low  $\text{CO}_2$  conversion and methanol yield (<50%). Therefore, the development of highly active and selective catalysts, as well as the optimisation of NTP reactor design, is necessary to further improve NTP-enabled catalytic  $\text{CO}_2$  conversion to methanol. Men *et al* [53] prepared a highly dispersed Pt/film/ $\text{In}_2\text{O}_3$  catalyst via the plasma-assisted peptide-assembly method and used it for NTP-assisted  $\text{CO}_2$  hydrogenation, achieving a high  $\text{CO}_2$  conversion rate of  $\sim 37\%$  with a methanol selectivity of  $\sim 62.6\%$  due to the high Pt dispersion. Additionally, based on modelling, Iliuta *et al* [54] proposed an integrated reactor for converting  $\text{CO}_2$  to methanol which involved the RWGS reaction under plasma conditions and subsequent catalytic methanol synthesis via CO and  $\text{CO}_2$  hydrogenation under thermal conditions. The findings from the modelling suggest that methanol yield could be improved if  $\text{CO}_2$  is progressively substituted by CO via RWGS in the plasma reactor, potentially leading to enhanced  $\text{CO}_2$  conversion and an increase in the overall energy efficiency.

#### 2.4. $\text{CO}_2$ reforming

In addition to  $\text{H}_2$ ,  $\text{CH}_4$  and  $\text{H}_2\text{O}$  can also be used as the H source for converting  $\text{CO}_2$  into value-added compounds. Activation of  $\text{CH}_4$  molecules is also energy intensive ( $600^\circ\text{C}\text{--}1100^\circ\text{C}$ ) due to the stable C–H bonds ( $E_{\text{diss}} = 4.5\text{ eV}$ ) [55]. From a thermodynamic point of view, the co-conversion of the greenhouse gases  $\text{CO}_2$  and  $\text{CH}_4$

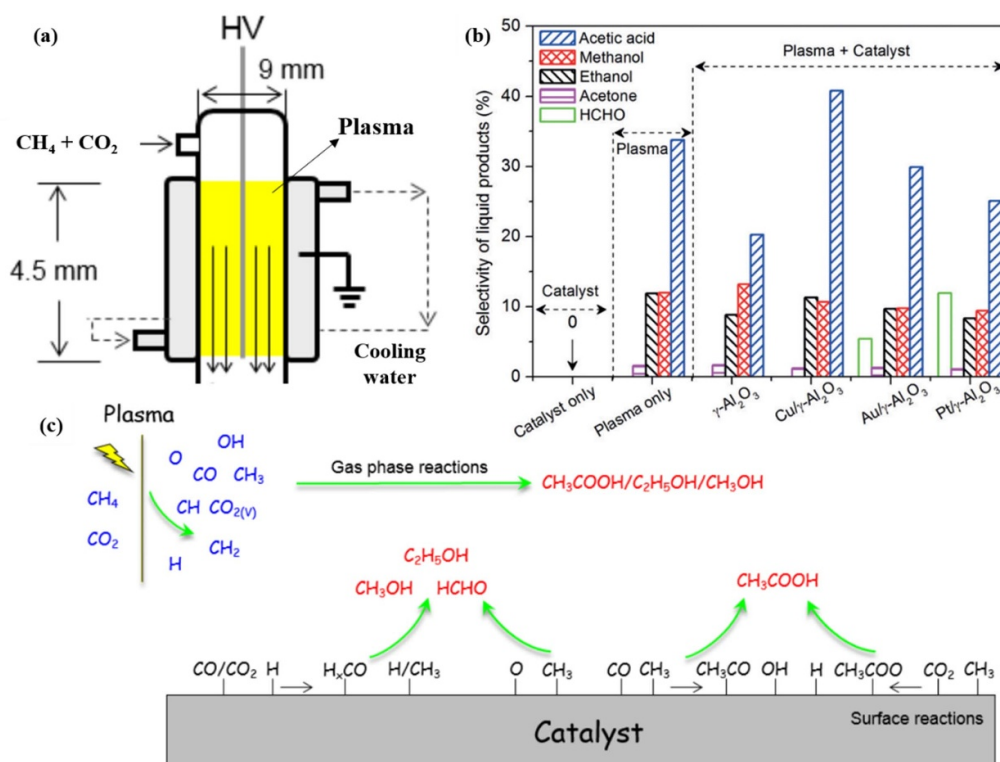


**Figure 3.** (a) The reactor configuration for one-step plasma-assisted DRM for producing liquid chemicals/fuels. (b) Selectivity to oxygenates and (c) possible reaction mechanisms for the formation of  $\text{CH}_3\text{COOH}$ ,  $\text{CH}_3\text{OH}$ ,  $\text{C}_2\text{H}_5\text{OH}$  and  $\text{HCHO}$  using NTP catalysis. Reprinted from [63]. CC BY 4.0.

(i.e. dry reforming of methane, DRM) cannot occur at low temperatures because of negative Gibbs free energy [56]. Alternatively, NTPs can overcome the thermodynamic limitation without the issues of coke formation and metal sintering experienced by thermal catalysis [55–57]. The target product of DRM is syngas ( $\text{CO} + \text{H}_2$ ), but hydrocarbons can also be produced [58, 59], depending on the selectivity of the catalyst, as well as other process parameters. For example, reaction selectivity was found to be sensitive to the gas composition [11, 60, 61], with a  $\text{CH}_4$ -rich feed contributing to high selectivity towards hydrocarbons, whilst the  $\text{CO}_2$ -rich feed increased  $\text{CO}$  selectivity [61].

NTPs combined with a suitable catalyst can tune reaction selectivity towards valuable hydrocarbons and liquid oxygenates. For example, the selectivity of DRM to  $\text{C}_2$  to  $\text{C}_4$  hydrocarbons was enhanced over NaX zeolite catalysts under NTP conditions [60]. Similarly, Vakili *et al* [62] reported that the combination of NTP with the UiO-67 metal–organic framework (MOF) facilitated the formation of  $\text{C}_2\text{H}_2$  and  $\text{C}_2\text{H}_4$ , whereas the  $\text{Pt}/\text{UiO-67}$  catalyst decreased the selectivity to hydrocarbons by  $\sim 30\%$  due to the dehydrogenation process on the Pt surface. Recently, Wang *et al* [63] demonstrated one-step synthesis of liquid chemicals/fuels including acetic acid, methanol, ethanol and formaldehyde from NTP-assisted DRM (as shown in figure 3) by careful selection of catalysts and operation parameters. The NTP-only system promoted the formation of oxygenates (selectivity of 59.1%), with acetic acid as the major product. In contrast, by varying the

catalysts within the DBD reactor, the distribution of liquid products could be tuned due to the presence of both gas-phase and plasma-assisted surface reactions. For example, the  $\text{Cu}/\gamma\text{-Al}_2\text{O}_3$  catalyst increased selectivity to acetic acid to  $\sim 40.2\%$  as compared with a plasma system with the  $\gamma\text{-Al}_2\text{O}_3$  packing ( $\sim 20.2\%$ ). Conversely, supported noble metal catalysts (i.e.  $\text{Au}/\gamma\text{-Al}_2\text{O}_3$  and  $\text{Pt}/\gamma\text{-Al}_2\text{O}_3$ ) produced formaldehyde under NTP conditions, suggesting that the nature of the catalysts is crucial for NTP catalysis (as shown in figure 3(b)). Optical emission spectral (OES) characterisation of the NTP catalysis system shows the presence of  $\text{CO}$ ,  $\text{CH}$ ,  $\text{CH}_3$ ,  $\text{CO}_2$ ,  $\text{CO}_2^+$ ,  $\text{OH}$  and  $\text{H}_\alpha$  as potential key species in the NTP-activated DRM. Therefore, possible reaction pathways on the catalyst surface for producing oxygenates have been proposed, as shown in figure 3(c), demonstrating the effect of the NTP-assisted surface reactions on the distribution of liquid products. This study confirms that NTP combined with heterogeneous catalysts can provide selective pathways to value-added products which cannot be achieved in NTP-only conditions.

$\text{CO}_2$  reforming with  $\text{H}_2\text{O}$ , mimicking the natural photosynthesis process, is very attractive since  $\text{H}_2\text{O}$  is the cheapest H source. The DBD reactor (without a catalyst) with the discharge gas of  $\text{CO}_2/\text{H}_2\text{O}$  mainly produces reactive species of  $\text{OH}$ ,  $\text{CO}$ ,  $\text{O}$  and  $\text{H}$ . However, the  $\text{OH}$  radicals are prone to recombine with  $\text{CO}$  molecules to produce  $\text{CO}_2$  and  $\text{H}$  atoms (thereby reducing  $\text{CO}_2$  conversion).  $\text{H}$  atoms can react with  $\text{O}$  to give  $\text{H}_2\text{O}$ , instead of forming  $\text{CH}$  and  $\text{CHO}$  species, which

are key intermediates in the production of oxygenated products [64]. Accordingly, NTP-only is not selective to oxygenated hydrocarbons in CO<sub>2</sub> reforming with H<sub>2</sub>O. Therefore, recent efforts have been dedicated to developing catalytic reforming systems using CO<sub>2</sub>/H<sub>2</sub>O plasma. Ma *et al* [65] demonstrated that the yields of H<sub>2</sub> and CO were significantly improved to 13.8% and 5.6%, respectively, when a Ni/ $\gamma$ -Al<sub>2</sub>O<sub>3</sub> catalyst was used in a DBD reactor as compared with NTP-only conditions. Zhao *et al* [66] also showed an enhanced ethanol production rate at 15.60  $\mu\text{mol g}_{\text{cat}}^{-1} \text{h}^{-1}$  using a Cu/ZnO/Al<sub>2</sub>O<sub>3</sub> catalyst under NTP conditions, which was much higher than that of the thermal system (with the catalyst, at 3.02  $\mu\text{mol g}_{\text{cat}}^{-1} \text{h}^{-1}$ ) and NTP-only conditions (at 3.5  $\mu\text{mol g}_{\text{cat}}^{-1} \text{h}^{-1}$ ).

### 3. Catalyst design for NTP catalytic CO<sub>2</sub> conversion

As discussed above, the NTP itself can activate CO<sub>2</sub> at low temperatures without catalysts but is non-selective due to collisions between active species. Conversely, the surface reactions involved in NTP catalysis can stabilise reaction intermediates and change the reaction pathways to promote CO<sub>2</sub> conversion and selectively, directing the conversion to the target products. Therefore, the hybrid NTP catalysis system is very promising for improving CO<sub>2</sub> conversion and addressing the selectivity issue. Thus, the investigation into the role of the intrinsic nature of catalysts in selective CO<sub>2</sub> conversion under NTP conditions is important, i.e. rational design of bespoke catalysts with desirable textual, compositional and structural properties tailored for a specific NTP catalytic CO<sub>2</sub> conversion. However, relevant investigations and fundamental design principles regarding this aspect are still lacking, and the current catalysts used in NTP catalysis are still those which were designed for thermal catalysis. Here, the recent progress of the catalysts used for thermal catalytic CO<sub>2</sub> conversion will be briefly discussed first; then a strategy for designing specific heterogeneous catalysts for NTP catalysis will be proposed.

#### 3.1. Catalysts for thermally activated CO<sub>2</sub> conversion

Under thermal conditions, group 8–10 metals (e.g. Ru, Rh, Pd, Ni, Co, Fe) have been demonstrated to be efficient for CO<sub>2</sub> hydrogenation [67, 68]. Ni-based catalysts are the most widely used catalysts for CO<sub>2</sub> conversion due to their cost-effectiveness and high activity. However, the main issue of the Ni-based catalysts is their stability, especially at high reaction temperatures, because the Ni catalysts are prone to deactivation due to carbon deposition and metal sintering. Ni particle sintering can reduce the metal surface area and overall CO<sub>2</sub> adsorption capacity, and hence lead to deactivation (of the Ni/AlO<sub>x</sub> catalyst) [69]. In comparison, Rh- and Ru-based catalysts are relatively stable and show higher activity than the Ni-based counterparts. However, their limited availability and relatively high price make them less attractive for applications at a large scale. Recently, efforts have been made to study the influence of the metal particle size and dispersion on the catalyst performance in order to develop more efficient catalysts for CO<sub>2</sub> conversion [70]. For example, Guo *et al* [71] investigated the effect of Ru particle size (i.e. single Ru

atoms, nanoclusters ( $\sim 1.2$  nm) and nanoparticles ( $\sim 4$  nm)) of Ru/CeO<sub>2</sub> catalysts on CO<sub>2</sub> hydrogenation. Compared with single Ru atoms, the nanoclusters and nanoparticles showed weaker metal–support interactions, thus promoting the activation process; however, they showed higher H spillover, thus inhibiting the removal of H<sub>2</sub>O from the catalyst surface. The trade-off between these two factors led to the nanoclusters achieving the highest activity at 190 °C, with a turnover frequency (TOF) of  $7.41 \times 10^{-3} \text{ s}^{-1}$  and 98%–100% selectivity to CH<sub>4</sub>. Similarly, the correlation between product selectivity and Ru particle size was studied by Kwak *et al* [72] and Yan *et al* [73]. It was revealed that single Ru atoms tend to form CO via RWGS, whereas Ru nanoclusters and nanoparticles favour the production of CH<sub>4</sub>. Regarding Ni catalysts, well-dispersed Ni particles are beneficial for the efficient conversion of CO<sub>2</sub> to CH<sub>4</sub>. For example, Ni nanoparticles of 2.7–4.7 nm (confined in the cage-type mesopores of SBA-16) enabled strong adsorption of CO<sub>2</sub> and high catalytic rates in CO<sub>2</sub> hydrogenation [74]. High Ni dispersion can be achieved by using porous catalyst supports, such as structured silica, zeolite and MOFs, with large surface areas and/or micro-/meso-porosity structures [75]. For example, UiO-66 MOF with a large surface area of 986 m<sup>2</sup> g<sup>-1</sup> was used as a support to prepare highly dispersed Ni with an average particle size of 2 nm for CO<sub>2</sub> methanation with good activity (TOF = 0.04 s<sup>-1</sup> at 320 °C) and stability (100 h) [76].

The surface properties of catalyst supports are also very important because (a) support–metal interactions can tune the properties of metals, such as the reducibility of metal species, metal dispersion and particle size and (b) basicity/acidity and oxygen vacancy can influence CO<sub>2</sub> adsorption. Different supports, including Al<sub>2</sub>O<sub>3</sub> [77–79], SiO<sub>2</sub> [80], TiO<sub>2</sub> [81], ZrO<sub>2</sub> [82], CeO<sub>2</sub> [83] and zeolites [84], have been applied to prepare catalysts for CO<sub>2</sub> conversion. Lin *et al* [82] found that Zr doping of Ni/Al<sub>2</sub>O<sub>3</sub> catalysts can improve Ni dispersion and the reducibility of the Ni phase, thus promoting CO<sub>2</sub> hydrogenation at low temperatures, of <300 °C. Le *et al* [85] investigated CO<sub>2</sub> methanation over the supported Ni catalyst on various supports and the activity was found to take place in the following order: CeO<sub>2</sub> > ZrO<sub>2</sub> > SiO<sub>2</sub> > Al<sub>2</sub>O<sub>3</sub> > TiO<sub>2</sub>. The high catalytic activity of the Ni/CeO<sub>2</sub> catalyst was attributed to the small Ni particle size, as well as the presence of oxygen vacancy, which facilitated CO<sub>2</sub> chemisorption and activation [86, 87]. Operando diffuse reflectance infrared Fourier transform spectroscopy (DRIFTS) studies of CO<sub>2</sub> hydrogenation over Ru/CeO<sub>2</sub> (with oxygen vacancy) and Ru/Al<sub>2</sub>O<sub>3</sub> (without oxygen vacancy) catalysts showed that the oxygen vacancy in CeO<sub>2</sub> facilitated the dissociation of formate species for CH<sub>4</sub> formation [88]. Additionally, a mechanistic investigation of CO<sub>2</sub> hydrogenation over the Ni/CeO<sub>2</sub> catalysts by Cárdenas-Arenas *et al* [89] and Ye *et al* [90] also showed that, in these catalysts, the existence of both Ni<sup>0</sup> sites (for H<sub>2</sub> dissociation) and Ce<sup>3+</sup> sites (for CO<sub>2</sub> adsorption and activation) was important to enable the selective CO<sub>2</sub> conversion to CH<sub>4</sub>. Therefore, developing next-generation catalysts with highly dispersed metal active sites, a large surface area and enhanced CO<sub>2</sub> adsorption is important for improving thermal catalytic CO<sub>2</sub> conversion, especially at low temperatures (<300 °C).

[91]. An understanding of the structure–composition–activity correlation in thermal catalysis will provide useful guidance for NTP catalysis systems in designing highly selective catalysts in order to improve the performance of hybrid systems.

### 3.2. Role of metal active sites in NTP catalytic CO<sub>2</sub> conversion

In thermal catalysis, reactions occur only on the catalyst surface, and the highly dispersed catalysts on appropriate supports can convert CO<sub>2</sub> effectively. In contrast, in plasma catalysis, the combination of gas-phase and surface reactions, complex interactions between plasma and catalysts such as plasma discharge properties, transport of reactive species and modification of catalysts by plasma are coupled to one another, all affecting the performance of hybrid systems.

Table 1 summarises the performance of various supported metal catalysts in NTP-assisted CO<sub>2</sub> hydrogenation. Clearly, the combination of plasma and catalysis can effectively improve CO<sub>2</sub> conversion. CO<sub>2</sub> hydrogenation over the Cu/Al<sub>2</sub>O<sub>3</sub>, Mn/Al<sub>2</sub>O<sub>3</sub> and Cu–Mn/Al<sub>2</sub>O<sub>3</sub> catalysts was carried out, showing CO<sub>2</sub> conversion enhanced by 6.7%–36% as compared with the NTP-only system [92]. As was found for thermal systems, Ru and Ni catalysts have been widely used for CO<sub>2</sub> hydrogenation under NTP and have shown improved CO<sub>2</sub> conversion (generally >50%) compared with that achieved by plasma-only systems. Other metals, such as Pt, Pd, Co, Fe and Cu, have also been explored for NTP catalytic CO<sub>2</sub> hydrogenation. Oshima *et al* [93] investigated Pt, Pd, Ni, Fe and Cu metals supported on La–ZrO<sub>2</sub> for NTP-activated CO<sub>2</sub> hydrogenation, in which the noble metals showed improved CO<sub>2</sub> conversion than using transition metal catalysts. It was also found that the Pt, Pd, Fe and Cu catalysts for CO<sub>2</sub> hydrogenation were selective to CO, whilst the Ni catalysts were CH<sub>4</sub> selective [42, 94]. Additionally, the Ni particle size and dispersion were also found to affect catalyst performance. Liu *et al* investigated CO<sub>2</sub> hydrogenation over Ni/La<sub>2</sub>O<sub>3</sub> catalysts as a function of calcination temperature from 600 °C to 900 °C. A maximum CO selectivity of 78% was achieved with the Ni/La<sub>2</sub>O<sub>3</sub> catalyst calcined at 600 °C, which was due to the small Ni particle size (~7.3 nm) and the high Ni dispersion achieved under the specific preparation conditions [95].

NTPs can facilitate catalyst preparation, resulting in the formation of small and highly dispersed metal nanoparticles on the support [99]. For example, H<sub>2</sub> plasma reduction was used to prepare the Pd, Pt, Ag and Au supported on SBA-15 catalysts, which showed improved activity in catalytic CH<sub>4</sub> conversion to value-added fuels [100]. Characterisation of these catalysts confirmed that the plasma treatment resulted in high metal dispersion; e.g. the particle sizes of Pd, Pt and Au were 6, 2 and 6 nm, respectively, which were able to fit into the ordered SBA channels (average diameter of 7.6–8.5 nm). Benrabbah *et al* [42] compared the effect of thermal and H<sub>2</sub> plasma reduction on the preparation of Ni/CeZrO<sub>2</sub> catalysts for plasma catalytic CO<sub>2</sub> hydrogenation, showing that the catalysts reduced by H<sub>2</sub> plasma resulted in a strong interaction between Ni and ceria, thus leading to higher CO<sub>2</sub> conversion

(~80%) at low power (~5 W) than the catalysts reduced by the thermal treatment (at 470 °C). These studies demonstrate that it is promising to employ the plasma reduction process to prepare highly dispersed metal catalysts *in situ* for NTP catalysis.

### 3.3. Role of catalyst supports in NTP catalytic CO<sub>2</sub> conversion

The properties of the catalyst support (e.g. morphology, dielectric properties and pore structures) are important in NTP catalysis as they affect metal dispersion, adsorption/desorption properties and plasma discharge. A summary of Ni catalysts supported on various supports for NTP catalytic CO<sub>2</sub> hydrogenation is presented in table 2.

**3.3.1. Catalysts supported on metal oxides.**  $\gamma$ -Al<sub>2</sub>O<sub>3</sub> is the most common support used for NTP-assisted CO<sub>2</sub> conversion due to its relatively large surface area (~150 m<sup>2</sup> g<sup>-1</sup>) and high stability [47]. However, the acidic nature of  $\gamma$ -Al<sub>2</sub>O<sub>3</sub> suppresses CO<sub>2</sub> adsorption, and hence CO<sub>2</sub> conversion over the catalysts supported on  $\gamma$ -Al<sub>2</sub>O<sub>3</sub> is relatively low in NTP catalysis. For example, in the NTP-assisted DRM, the Ni/ $\gamma$ -Al<sub>2</sub>O<sub>3</sub> catalyst achieved a CO<sub>2</sub> conversion rate of 26.2% and CH<sub>4</sub> conversion rate of 44.1% [107], and in NTP catalytic CO<sub>2</sub> methanation (as shown in table 1), only 23% CO<sub>2</sub> conversion was achieved by the Ru/ $\gamma$ -Al<sub>2</sub>O<sub>3</sub> catalyst [46]. Catalyst supports with basic sites and oxygen vacancies have also been explored for NTP catalytic CO<sub>2</sub> conversion. For example, Nizio *et al* [8, 101] developed Ni catalysts supported on CeZrO<sub>2</sub> with different Ce/Zr ratios for NTP-assisted CO<sub>2</sub> hydrogenation. The highest CO<sub>2</sub> conversion rate of ~80% and CH<sub>4</sub> selectivity of ~95% was achieved when the Ce/Zr ratio was 1.40. In these catalysts, ceria acted as an oxygen reservoir, which promoted the adsorption of CO<sub>2</sub> and subsequently produced CO and O active species with the assistance of plasma. Recently, hydrotalcite-derived/-supported metal catalysts have shown potential in C1 chemistry due to their compositional flexibility, good thermal stability and basic properties, which facilitates chemisorption and activation of CO<sub>2</sub> [108]. Additionally, the coordinatively unsaturated active sites in hydrotalcite such as steps, edges and corner atoms can also promote metal dispersion, favouring catalysis [109]. Xu *et al* [110] prepared Ru supported on MgAl-layered double hydroxide catalysts for NTP-assisted CO<sub>2</sub> hydrogenation, in which ~85% CO<sub>2</sub> conversion and ~84% CH<sub>4</sub> yield were achieved.

**3.3.2. Catalysts supported on zeolites.** Zeolites have been widely used for heterogeneous catalysis due to their uniform micropores, large surface areas, tunable acidities and high thermal stabilities [111]. Zeolites also have the ability to spatially confine reactions, thus preventing the aggregation and deactivation of metallic species [112]. Zeolite-supported Ni catalysts have been explored for CO<sub>2</sub> hydrogenation under NTP conditions. Bacariza *et al* [106] evaluated NTP-assisted CO<sub>2</sub> methanation over a Ni/USY zeolite catalyst and investigated the effect of the Si/Al ratio and Ce addition on catalytic

**Table 1.** Comparison of NTP-assisted catalytic CO<sub>2</sub> hydrogenation over different catalysts.

Catalysts	DBD power (W)	WHSV <sup>a</sup> (ml g <sub>cat</sub> <sup>-1</sup> h <sup>-1</sup> )	CO <sub>2</sub> conv. (%)			CO <sub>2</sub> rate (mol s <sup>-1</sup> g <sup>-1</sup> , ×10 <sup>-3</sup> )	CH <sub>4</sub> yield (%)	CO yield (%)	Ref.
			NTP only	Catalyst (thermal) <sup>b</sup>	NTP + catalyst				
6% Ru/γ-Al <sub>2</sub> O <sub>3</sub>	33	18 625	8.2	0.01 (at 25 °C)	23	0.06	—	—	[46]
2% Ru/UiO-66	13	—	22	—	41	—	—	—	[96]
2.8% Ru@UiO-66	13	6000	20	—	72	0.11	—	—	[97]
15% Ni/Ce <sub>x</sub> Zr <sub>1-x</sub> O <sub>2</sub>	>13	20 000	—	—	80	0.26	—	—	[42]
10% Ni/γ-Al <sub>2</sub> O <sub>3</sub>	15–18	20 000	9	2 (at 150 °C)	60	1.5	—	—	[47]
Ni/La <sub>2</sub> O <sub>3</sub>	90	18 000	52	—	97	—	9.7	—	[95]
NiFe/MgAlO <sub>x</sub>	12	12 000	—	76 (at 250 °C)	73	0.08	—	—	[98]
8% Cu/γ-Al <sub>2</sub> O <sub>3</sub>	35	2076	7.5	—	8	0.01	0.7	6.4	[92]
8% Mn/γ-Al <sub>2</sub> O <sub>3</sub>	35	2076	—	—	10	0.02	0.76	7.9	[92]
2% Pd/ZnO	30	3600	19.8	1.5 (at 230 °C)	32.5	0.18	—	31.3	[94]
2% Pd/SiO <sub>2</sub>	30	3600	—	—	25.3	0.14	—	20.8	[94]
1% Pt/La–ZrO <sub>2</sub>	5.6	60 000	18	—	41	7.8	—	40.6	[93]
1% Pd/La–ZrO <sub>2</sub>	3.5	60 000	—	—	31	5.7	—	30.5	[93]
1% Fe/La–ZrO <sub>2</sub>	4.1	60 000	—	—	27	5.0	—	27.1	[93]

<sup>a</sup> WHSV; weight hourly space velocity.

<sup>b</sup> Catalyst (thermal); CO<sub>2</sub> conversion achieved by catalysts activated under thermal conditions at different temperatures for comparison.

**Table 2.** Comparison of the performance of CO<sub>2</sub> hydrogenation over Ni-supported on various supports in DBD reactors under NTP conditions.

Catalysts	DBD power (W)	WHSV (ml g <sub>cat</sub> <sup>-1</sup> h <sup>-1</sup> )	CO <sub>2</sub> conv. (%)			CH <sub>4</sub> selectivity (%)	CH <sub>4</sub> yield (%)	Ref.
			NTP only	Catalyst thermal <sup>a</sup>	NTP + catalyst			
15Ni–CeO <sub>2</sub> /Al <sub>2</sub> O <sub>3</sub>	15–40	40 000	3	4 (at 250 °C)	70	96	67	[45]
15Ni/Ce <sub>0.1</sub> Zr <sub>0.9</sub> O <sub>2</sub>	1–3	50 000	—	0 (at 280 °C)	80	99.7	79.8	[101]
15Ni–TiO <sub>2</sub> /Al <sub>2</sub> O <sub>3</sub>	—	1100	13	5 (at 220 °C)	50	—	—	[102]
15Ni/UiO66	1–3	30 000	5	5 (at 200 °C)	85	99	84.2	[103]
15Ni/CZ/SBA-15	—	20 000	—	<1 (at 200 °C)	80	99	79	[104]
15NiLa/Na–BETA	1–3	23 007	10	0 (at 200 °C)	84	97	81	[105]
NiCe/CS–USY	35	40 000	<5	20 (at 250 °C)	79	98	77	[106]

<sup>a</sup> Catalyst (thermal): CO<sub>2</sub> conversion achieved by catalysts activated under thermal conditions at different temperatures for comparison.

performance. It was found that a higher Si/Al ratio could lead to lower affinity towards water, reducing the inhibiting effect of H<sub>2</sub>O on catalyst activity in CO<sub>2</sub> methanation. The addition of Ce as promoter in the Ni/USY catalyst favoured CO<sub>2</sub> activation and improved the dielectric constant of the catalyst ( $\epsilon_r = 24$  for CeO<sub>2</sub> versus  $\epsilon_r = 1.5$ – $5$  for zeolites), leading to high CO<sub>2</sub> conversion ( $\sim 70\%$ ) and CH<sub>4</sub> yield ( $\sim 75\%$ ). Chen *et al* [105] investigated the performance of BETA zeolite-supported Ni catalysts in NTP-assisted catalytic CO<sub>2</sub> hydrogenation. It was found that, as compared with H-form BETA, Na-form BETA benefits CO<sub>2</sub> adsorption, which can be further improved by La doping.

Additionally, the effect of porous catalysts on plasma discharge properties also deserves attention. Both experimental and modelling studies have shown that the pore structure of catalysts can intensify the electric field due to the formation of strong micro-discharges [20, 113]. A two-dimensional (2D) fluid model predicted that plasma could be formed and penetrate pores with a pore diameter greater than the Debye length (typically  $>2 \mu\text{m}$ ) [114, 115]. Although the average pore size of zeolites is much smaller than the Debye length, a previous study based on Monte Carlo calculations revealed that micro-discharges might be formed near the pores of micro-/mesoporous catalysts, thus promoting intensified surface discharges on the porous catalyst [116]. Therefore, an understanding of the relevant discharge characteristics of the NTP catalysis is important in order to gain insights into the NTP catalyst interactions and further develop NTP catalytic systems. On the other hand, the lifetimes of plasma-induced reactive species are short, ranging from a few nanoseconds (for electronically excited atoms/molecules) to microseconds (for radicals) [117, 118]. Thus, the plasma-induced reactive species may lose their energy due to collisional quenching before participating in surface reactions. Accordingly, the diffusion of short-lived reactive species to the active sites is a key parameter in determining the efficiency of plasma catalysis, and an understanding of the diffusion mechanisms within the porous network of the catalysts is necessary for NTP catalysis [22]. Recently, Chen *et al* [119] investigated how the catalyst structure, for example the location of the active sites and support pore structures, affects

the diffusion of the reactive species and the catalytic performance in CO<sub>2</sub> hydrogenation by designing a series of Ni supported on silicalite-1 (with different pore structures) catalysts (as shown in figure 4). Specifically, at low input energy, the availability of NTP-reduced reactive species in the gas phase is limited, and thus they prefer to interact with the exposed Ni active sites on the external surface of the catalysts with less diffusion resistance. Conversely, at high input energy, the abundant presence of the reactive species enables diffusion into the pore of the zeolite and allows interactions with the highly dispersed active sites. Thus, catalysts with a hierarchical meso-/micro-porous network and the associated highly dispersed Ni species may benefit the accessibility of short-lived reactive species towards Ni active sites, leading to the relatively high CO<sub>2</sub> conversion rate of  $\sim 75\%$ . This work demonstrates that the intrinsic nature of catalysts (e.g. pore structure, metal dispersion and the location of active sites) plays a key role in NTP catalysis, and the development of catalysts with highly dispersed and easily accessible metal sites may benefit NTP catalysis towards practical applications.

**3.3.3. Catalysts supported on MOFs.** MOFs have exceptionally large specific surface areas, structural diversity and tailorability, tunable pore size distribution and confined microenvironment, which enable flexible catalyst design by allowing active guest species to be anchored into their pores/cages/channels [120]. However, under thermal conditions, catalysts based on MOFs are often unstable. This can potentially be solved by using NTP activation. In addition, it is well known that MOFs have much stronger CO<sub>2</sub> adsorption capacities than other materials, such as zeolites and silica, which has inspired the development of MOF-based catalysts for CO<sub>2</sub> fixation and conversion under NTP conditions [121]. Chen *et al* [103] developed a Ni support on UiO-66 catalysts for catalytic CO<sub>2</sub> hydrogenation under NTP conditions. The TOF of the NTP catalysis system had a nearly two-fold improvement as compared with thermal catalysis ( $1.8 \text{ s}^{-1}$  vs.  $0.06 \text{ s}^{-1}$ ) and the structure of the catalyst showed no significant change after 20 h testing, confirming that the high

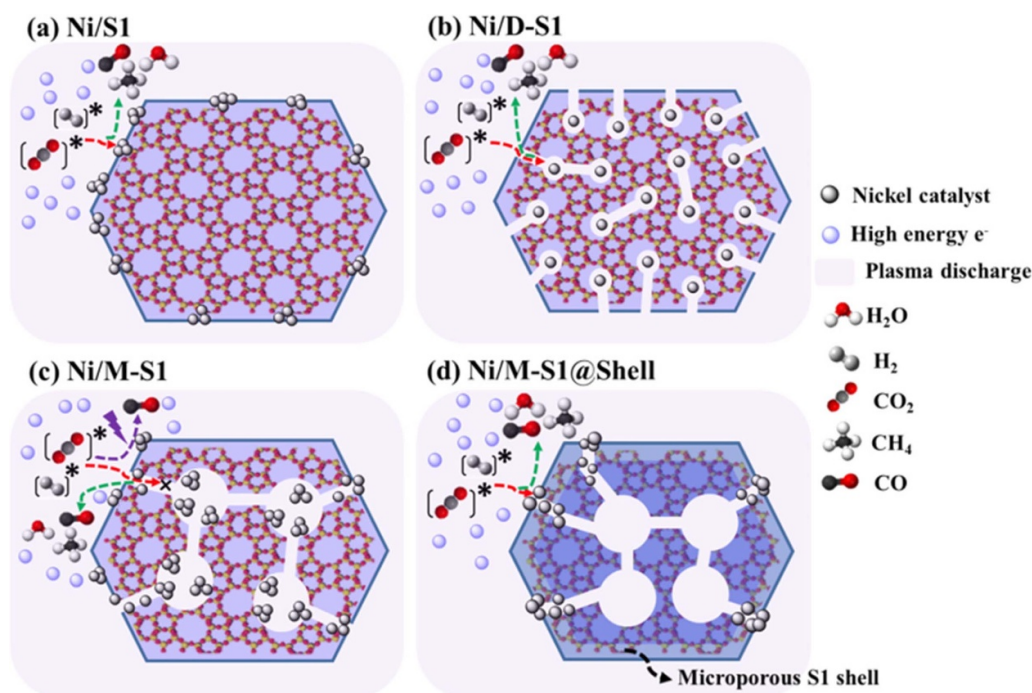


**Figure 4.** Mechanistic scheme of catalysts with different pore structures for NTP-assisted CO<sub>2</sub> hydrogenation. Reprinted from [119]. Copyright (2020), with permission from Elsevier.

stability of the MOF-based catalyst under NTP conditions can be achieved. Vakili *et al* [62] investigated the performance of the Pt@UiO-67 catalyst in the plasma-assisted DRM. Therein, it was found that, in addition to the high stability of the catalyst, the large surface area and the porous structure of UiO-67 also favoured the formation of micro-discharges on the catalyst surface, improving the conversion of CH<sub>4</sub> and CO<sub>2</sub> by 18% and 10%, respectively. These studies demonstrate the potential of MOF-based catalysts to improve NTP catalysis, as well as the use of NTP activation to sustain MOF-based catalyst activity. However, to date, the bespoke design of MOF-based catalysts for NTP-assisted CO<sub>2</sub> conversion and the relevant mechanistic understanding are lacking, requiring further investigation.

**3.3.4. Promoter modified supported catalysts.** The addition of promoters such as alkali and rare-earth metal oxides to metal-supported catalysts has been shown to be effective in improving metal dispersion and reducibility as well as the acid/base properties of the catalysts, resulting in the enhanced activity and stability of catalysts under thermal activation [122–124]. Accordingly, relevant research on the evaluation of promoter-modified catalysts in plasma catalytic CO<sub>2</sub> conversion has been conducted, as shown in table 3. Khoja *et al* [59] found that the La-promoted Ni/MgAl<sub>2</sub>O<sub>4</sub> catalysts improved CO<sub>2</sub>/CH<sub>4</sub> conversion to 84.5% and 86%, respectively, in the NTP-assisted DRM. Similarly, Chen *et al* [105] developed La-promoted Ni/Na–BETA zeolite catalysts for CO<sub>2</sub> hydrogenation, which showed improved CO<sub>2</sub> conversion (in comparison with the Ni/Na–BETA zeolite catalyst) under NTP conditions. Ray *et al* [125] compared the performance of the MgO- and CeO<sub>2</sub>-promoted Ni/ $\gamma$ -Al<sub>2</sub>O<sub>3</sub> catalysts for NTP-assisted DRM.

The results showed that the MgO-promoted catalyst had the smallest particle size ( $\sim 12$  nm) and the largest surface area ( $\sim 201$  m<sup>2</sup> g<sup>-1</sup>) with a uniform distribution of Ni on the surface of the catalyst, leading to better catalytic performance with 34.7% and 13% conversion of CH<sub>4</sub> and CO<sub>2</sub>, respectively, as compared with the NTP system with Ni/ $\gamma$ -Al<sub>2</sub>O<sub>3</sub>. In comparison, the CeO<sub>2</sub>-promoted catalysts provided oxygen vacancy for CO<sub>2</sub> activation, resulting in improved anti-carbon deposition and maximum selectivity to CO. The effect of the promoters depends on their distribution and loading. Excessive addition of the promoters may block active sites, leading to a decrease in catalytic activity [126, 127]. On the other hand, Zeng *et al* [128] compared catalytic DRM over K-, Mg-, and Ce-promoted Ni/Al<sub>2</sub>O<sub>3</sub> catalysts under NTP and thermal conditions. Under thermal activation, the addition of the promoters reduced CH<sub>4</sub> conversion. Conversely, in NTP catalysis, the K-promoted catalyst improved CO<sub>2</sub>/CH<sub>4</sub> conversion, the yield of H<sub>2</sub>, CO and C<sub>2</sub>–C<sub>4</sub> alkanes and the energy efficiency of the system, whilst the Mg-promoted catalyst increased the H<sub>2</sub>/CO molar ratio due to decreased CO<sub>2</sub> conversion. This work suggests that catalysts presenting poor performance in thermal catalysis may perform well under NTP activation and vice versa. Therefore, fundamental research into the role of promoters in NTP catalysis and their mechanism of enhancement is needed to advance NTP catalysis.

#### 4. Mechanism of CO<sub>2</sub> conversion in NTP catalysis

Based on the discussion above, the rational design of bespoke catalysts for NTP catalysis is a key research direction which can enable efficient interaction between plasma and catalyst to improve the process efficiency of hybrid NTP catalysis

**Table 3.** Summary of NTP catalytic DRM over supported catalysts modified with various promoters.

Catalyst	Power (W)	CH <sub>4</sub> /CO <sub>2</sub>	CO <sub>2</sub> conv. (%)		CH <sub>4</sub> conv. (%)		Ref.
			NTP only	NTP + catalyst	NTP only	NTP + catalyst	
Ni–K/Al <sub>2</sub> O <sub>3</sub>	16	1.5		22.8		31.6	
Ni–Mg/Al <sub>2</sub> O <sub>3</sub>	16	1.5	18.2	15	25.1	22	[128]
Ni–Ce/Al <sub>2</sub> O <sub>3</sub>	16	1.5		21		32	
Ni/γ-Al <sub>2</sub> O <sub>3</sub> –MgO	100	1.0	58	73.5	64	74.5	[129]
Ni–Mn/γ-Al <sub>2</sub> O <sub>3</sub>	2.1	1.0	6	12	12	28.4	[58]
Na/La <sub>2</sub> O <sub>3</sub> –MgAl <sub>2</sub> O <sub>4</sub>	100	1.0	59	84.5	62	86	[59]
NiCeC	40	1.0	—	53.7	—	55.6	[127]
Ni/MgO–Al <sub>2</sub> O <sub>3</sub>	2.7	1.0	9.5	13	20	34.7	[125]
Ni/CeO <sub>2</sub> –Al <sub>2</sub> O <sub>3</sub>	2.7	1.0		12.1		30	

systems for CO<sub>2</sub> activation. Despite extensive studies performed to assess the overall performance of the selected catalysts for NTP catalytic CO<sub>2</sub> conversion, a fundamental understanding of the correlations between plasma, catalyst, plasma-induced reactive species and corresponding reaction mechanisms is still largely lacking.

Generally, NTP catalysis systems are highly complex including, not exhaustively, plasma discharge, ionisation/activation of molecules, adsorption/desorption process, surface reactions, species collisions, species transport in/between the gas and solid phase [21, 130]. Specifically, catalysts have been demonstrated to enhance the local electric field, affect the plasma discharge type and form microdischarges in porous catalysts, while the plasma may modify catalysts and their microscopic structure, metal dispersion and chemical state. Additionally, the interplay between catalyst and plasma-induced active species can be divided into (a) adsorption processes including the adsorption of neutral species, charge carriers and surface charging, and (b) surface reaction processes including photon-induced surface reactions and collision-induced surface reactions [24]. A higher adsorption ability and a lower activation barrier were observed in the case of plasma-induced vibrationally excited molecules due to the increasing energy of the reactants compared with the ground state, which may promote subsequent surface reactivity [20, 131]. The presence of free electrons and ions, i.e. free charges in the plasma state, could also improve the synergy of plasma catalysis by affecting the bond breaking and formation processes on the catalyst surface. For example, Jafarzadeh *et al* [132] investigated the effect of plasma-induced electrons on the adsorption and activation of CO<sub>2</sub> on titania-supported Cu<sub>5</sub> and Ni<sub>5</sub> clusters by using spin-polarised and dispersion-corrected density functional theory calculations. It was found that the electrons affected the adsorption process by shifting the antibonding states of CO<sub>2</sub> towards the valence band, increasing the polarisation effects and changing the adsorption site of CO<sub>2</sub>, which lead to improved stabilisation of dissociated CO<sub>2</sub> on the catalyst surface. On the catalyst surface, in addition to the electrons, plasma-produced photons may also induce electronic excitations, which in turn initiate catalytic surface reactions (i.e. photocatalysis). Plasma-induced photocatalysis has been proposed for catalytic VOC abatement over TiO<sub>2</sub>, in which 3.2 eV is required to excite an electron

in anatase TiO<sub>2</sub> [133]. However, other studies have demonstrated that the photocatalytic effect was negligible in plasma catalysis [134, 135]. Currently, the role of radiation in NTP catalytic CO<sub>2</sub> conversion has not yet been reported. Therefore, further research on the effect of photons on plasma catalytic systems is still needed. In collision-induced surface reactions, some energy may be delivered from the vibrational/electronically excited species and/or impinging photons and electrons to overcome the surface reaction barrier, thus lowering the activation barrier for surface reactions. On the catalyst surface, the surface reactions were demonstrated to proceed via the Langmuir–Hinshelwood or Eley–Rideal reaction mechanisms [136]. Therefore, a suite of comprehensive experimental methods including *in situ* techniques and computational/numerical investigations of plasma catalysis systems are required to provide fundamental insights into the behaviours of the reactive species in the gas phase and/or on the catalytic surface for these reactions.

OES is an important technique used to measure electron temperature and identify, *in situ*, reactive species in the gas phase, which can facilitate an understanding of the relevant reaction mechanisms. Various activated species such as H radicals, CO, CH, OH, C, CHO, CO<sub>2</sub> and CO<sub>2</sub><sup>+</sup> have been detected in NTP-assisted CO<sub>2</sub> hydrogenation, confirming that the plasma can activate relevant molecules for catalysis (as shown in figure 5) [46, 47, 137]. OES detection has also revealed direct collisions of reactive gas species with adsorbed species on the catalyst surface, showing the presence of the Eley–Rideal mechanism [47]. Since, in NTP catalysis, reactions occur simultaneously in the gas-phase and on the catalyst surface, decoupling the contribution of the gas-phase reactions from the surface reactions can be highly beneficial to our understanding of the mechanism of NTP catalysis, though it is highly challenging. A temperature-programmed plasma surface reaction (TPPSR) method was developed to study the plasma catalytic CO<sub>2</sub> hydrogenation, which can remove gas-phase CO<sub>2</sub> and weakly adsorbed surface species before surface reaction [138]. Using TPPSR in combination with isotopically labelled <sup>13</sup>CO<sub>2</sub> (pre-adsorbed on the Co/CeZrO<sub>4</sub> catalyst surface), the formation of <sup>12</sup>CH<sub>4</sub> was immediately observed whilst no <sup>13</sup>CH<sub>4</sub> was formed when the <sup>12</sup>CO<sub>2</sub>/H<sub>2</sub> plasma was ignited. This indicated that the gaseous CO<sub>2</sub> was dissociated to CO in the gas phase and subsequently reacted with H<sub>2</sub> on the

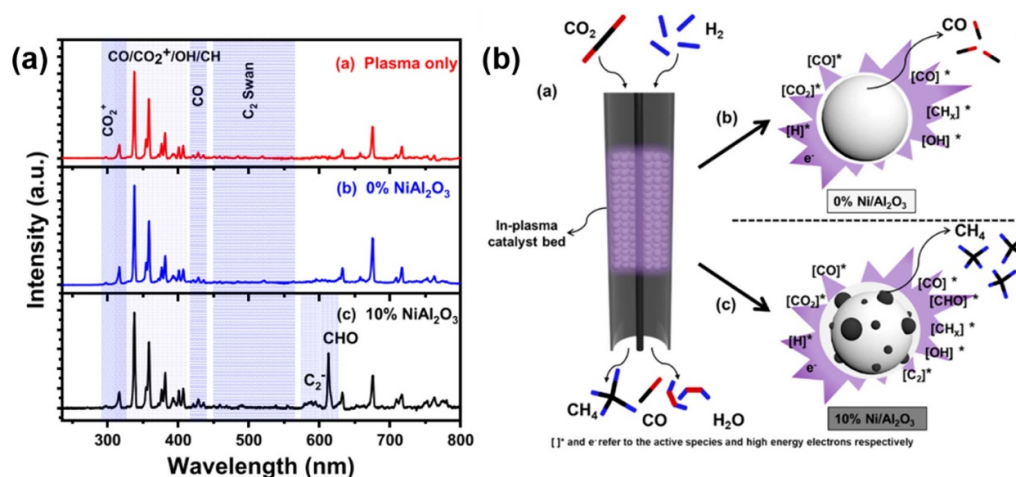


**Figure 5.** (a) Comparison of OES spectra in NTP catalytic CO<sub>2</sub> hydrogenation for three systems: plasma only, plasma discharge with Al<sub>2</sub>O<sub>3</sub>, and plasma discharge with 10% Ni/Al<sub>2</sub>O<sub>3</sub>; and (b) proposed scheme of plasma catalytic interaction for CO<sub>2</sub> hydrogenation over Ni catalysts. Reprinted with permission from [47]. Copyright (2020) American Chemical Society.

cobalt surface to enable CH<sub>4</sub> formation. This technique confirms that plasma-induced CO<sub>2</sub> dissociation in the gas phase can intensify catalyst performance at low temperatures.

Although OES can provide valuable information on the reactive species in the gas phase, direct measurements of the surface reactions on the microscopic scale under NTP conditions are also valuable. Thus, direct operando observation of catalyst structures regarding the evolution and the formation of active surface species using *in situ* techniques has been performed to elucidate and understand catalysis under NTP. Azzolina-Jury *et al* [139] employed microsecond time-resolved FTIR spectroscopy to study the intermediates of plasma-activated CO<sub>2</sub> hydrogenation over the Ni-USY catalysts. The findings showed that NTP-induced partial dissociation of CO<sub>2</sub> (to CO) contributed to gas-phase reactions, whilst, on the catalyst surface, the adsorption of vibrationally excited CO<sub>2</sub> contributed to the formation of formates, which were further hydrogenated into carbonyl species. They also found that CO in the gas phase can adsorb on the Ni surface to form reactive intermediates for CO<sub>2</sub> hydrogenation, demonstrating the existence of multiple pathways under NTP conditions. Recently, a DRIFTS technique (as shown in figure 6) was developed by Stere *et al* [140] for NTP catalysis to probe the dynamics of the surface species and intermediates on the catalyst surface, including selective catalytic reduction of NO<sub>x</sub> [141, 142], WGS [9, 10], CO<sub>2</sub> hydrogenation [103, 143] and DRM [62], which provided valuable information on the explanation of the possible mechanisms and reaction pathways using NTP catalysis. By combining *in situ* DRIFTS with the mass spectrometry study, Chen *et al* [105] confirmed the co-existence of Langmuir–Hinshelwood and Eley–Rideal mechanisms in NTP catalytic CO<sub>2</sub> hydrogenation, i.e. both the surface reactions (between the adsorbed species) and interactions between the adsorbed and gas-phase species contributed to the formation of CH<sub>4</sub>. Furthermore, Xu *et al* [110] revealed that NTP catalysis promoted more active species including CO<sup>\*</sup>, O<sup>\*</sup>, H<sup>\*</sup>, formates, carbonate,

formyl and carbonyl in comparison with the thermal counterpart, showing the presence of alternative reaction pathways for CO<sub>2</sub> hydrogenation in the NTP catalysis. A study using *in situ* DRIFTS for plasma-activated DRM over the Ni/Al<sub>2</sub>O<sub>3</sub> catalyst with La as a promoter also found that the vibrational states of CH<sub>4</sub> and plasma-induced CO<sub>2</sub> activation contributed to the improved performance of NTP catalysis [144]. Specifically, plasma could facilitate CO<sub>2</sub> activation to produce a 1.7-fold enhancement in surface carbonate formation on La as compared with thermal activation. The surface reaction between CH<sub>x</sub><sup>\*</sup> and carbonate species promoted improved CH<sub>4</sub> conversion in the plasma-assisted DRM.

In addition to *in situ* DRIFTS, *in situ* x-ray absorption fine structure (XAFS) has also been developed to characterise the structural changes of catalysts during NTP catalysis. CH<sub>4</sub> oxidation under NTP conditions was investigated by *in situ* monitoring of the x-ray adsorption fine structure of Pd/Al<sub>2</sub>O<sub>3</sub> catalysts [145]. It was found that, during the NTP catalysis, the catalyst did not show significant structural changes, and the plasma-induced heating of Pd nanoparticles was suggested, confirming the perturbation role of NTP in the hybrid system [22]. Although *in situ* XAFS characterisation has been applied to CO<sub>2</sub> hydrogenation under thermal conditions [146–148], it has not yet been used for NTP-assisted CO<sub>2</sub> hydrogenation. In summary, *in situ* characterisation is crucial for NTP catalysis as it will allow us to (a) identify the critical steps of surface reactions, (b) understand the catalyst changes during NTP catalysis, and (c) establish ideal NTP conditions that optimally exploit the NTP catalysis.

Kinetic studies are also a useful experimental method used to understand NTP catalyst interactions, allowing us to understand the effect of relevant variables, such as discharge power, reactant concentration and catalysts, on the chemical reaction (e.g. reaction rate and activation barrier) in order to maximise the efficiency of hybrid systems. The pioneering work of Kim *et al* [23] on the kinetic evaluation of CH<sub>4</sub> activation over the Ni catalyst in a thermal DBD plasma hybrid reactor,

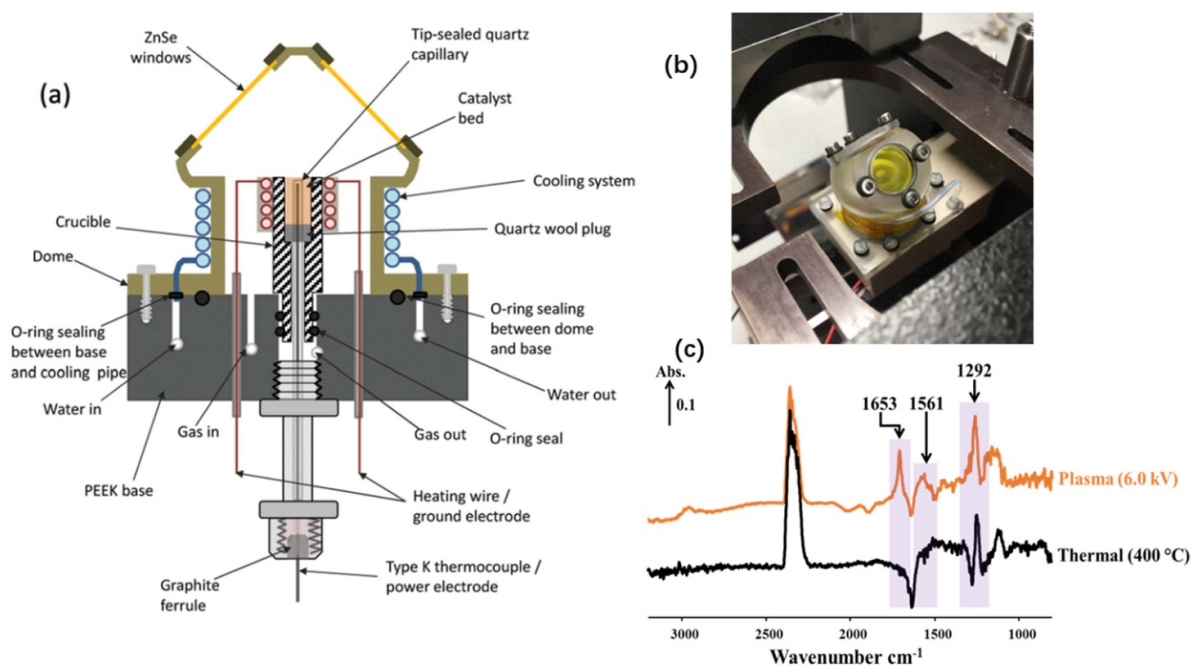


**Figure 6.** (a), (b) Schematic and photograph of *in situ* plasma flow cell for a DRIFTS study. Reproduced from [140] with permission of The Royal Society of Chemistry. (c) Comparison of *in situ* DRIFTS spectra of CO<sub>2</sub> hydrogenation under NTP and thermal conditions. Reproduced from [105] CC BY 4.0.

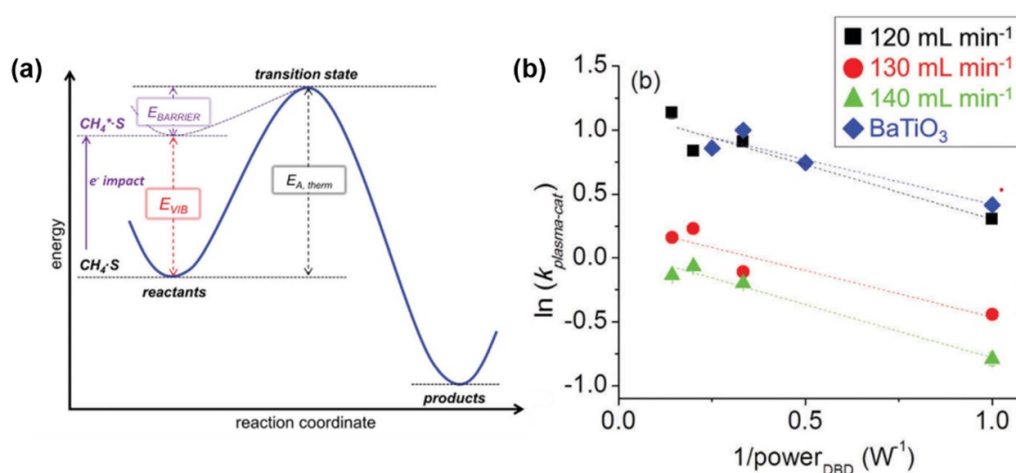


**Figure 7.** (a) Progress of thermal and plasma-assisted catalysis requiring energies of  $E_{A,therm}$  and  $E_{BARRIER}$  to reform CH<sub>4</sub> species at 790–890 K, respectively. (b) Logarithmic reaction rate constant ( $\ln k_{plasma-cat}$ ) vs.  $1/power_{DBD}$  under different reaction environments. Reproduced from [23] with permission of The Royal Society of Chemistry.

as shown in figure 7, established the correlation between the reaction rate and input power for calculation of the activation energy of NTP catalysis. Subsequently, a comparative kinetic study of CO<sub>2</sub> hydrogenation (over Ni@SiO<sub>2</sub>) under thermal and plasma activation was performed [137], showing that the activation energy of the NTP catalysis was estimated to be  $\sim 29$  kJ mol<sup>-1</sup>, which was significantly lower than that of the thermal catalysis ( $\sim 80$  kJ mol<sup>-1</sup>). These findings suggest that NTP activation can lower the activation barrier required to initiate catalysis.

In addition to experimental investigations, modelling and simulation of NTP catalysis have provided useful information

on relevant physical and chemical phenomena, as well as predicting the suitable catalysts and optimal conditions for NTP catalysis [149]. De Bie *et al* [150] investigated CO<sub>2</sub> hydrogenation in a DBD reactor using a one-dimensional fluid model (figure 8). It was found that CO and CH<sub>4</sub> were the main products of NTP catalysis, while the selectivity to methanol and hydrocarbons was relatively low, consistent with findings from experimental studies [50, 92]. The model suggests that the reaction starts with the electron impact dissociation of CO<sub>2</sub> and H<sub>2</sub> to form CO, O and H radicals. Further electron impact dissociation of CO then contributes to form the C, CH, CH<sub>2</sub>, and CH<sub>3</sub> radicals. The relatively low density of these

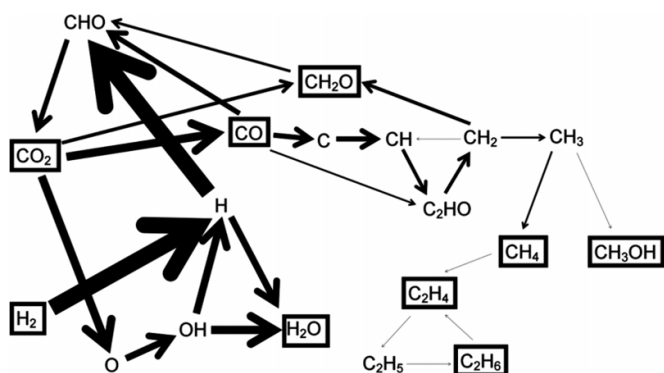


**Figure 8.** Dominant reaction pathways for the conversion of  $\text{CO}_2$  and  $\text{H}_2$  into various products proposed by the one-dimensional fluid model, in a 50/50  $\text{CO}_2/\text{H}_2$  gas mixture. Reprinted with permission from [150]. Copyright (2016) American Chemical Society.

radicals leads them to preferentially form  $\text{CH}_4$  rather than hydrocarbons and oxygenates (e.g.  $\text{C}_2\text{H}_6$ ,  $\text{C}_2\text{H}_4$  and  $\text{CH}_3\text{OH}$ ), explaining the low yield of hydrocarbons/oxygenates in  $\text{CO}_2$  hydrogenation. Recently, Stijn *et al* [151] developed a chemical kinetic model to study the underlying mechanism of conversion of  $\text{CO}_2$  and  $\text{CH}_4$  into hydrocarbons, especially  $\text{C}_2\text{H}_2$ ,  $\text{C}_2\text{H}_4$  and  $\text{C}_2\text{H}_6$ , under NTP conditions. The reaction was initiated by the electron-impacted dissociation/ionisation of  $\text{CH}_4$  to form  $\text{CH}_3$ ,  $\text{CH}_2$  and  $\text{CH}$  radicals. The coupling of  $\text{CH}_3$  mainly contributed to forming the  $\text{C}_2\text{H}_6$  product, while this process was counterbalanced by the electron impact dissociation/decomposition of  $\text{C}_2\text{H}_6$  to form  $\text{C}_2\text{H}_4$  and  $\text{C}_2\text{H}_2$ . Further dissociation and recombination of these  $\text{C}_2\text{H}_4$  and  $\text{C}_2\text{H}_2$  radicals led to the formation of higher hydrocarbons such as  $\text{C}_3\text{H}_8$ ,  $\text{C}_4\text{H}_{10}$  and  $\text{C}_5\text{H}_{12}$ . The simulation results showed that  $\text{CO}_2$  conversion with  $\text{CH}_4$  can directly form more  $\text{CH}_2$  and  $\text{CH}_3$  radicals by dissociation of  $\text{CH}_4$  in a plasma discharge, making it a potential route for producing hydrocarbons and oxygenates as compared with  $\text{CO}_2$  hydrogenation [152]. A 2D fluid model was developed by Zhang *et al* to investigate plasma formation inside porous catalysts with different pore sizes (in the range of 10–400  $\mu\text{m}$ ) and shapes (e.g. conical pores with small/large opening and cylindrical pores) in order to predict how the porous structure of catalysts affects plasma properties [113, 114]. These findings suggest that plasma micro-discharges may occur in pores with sizes larger than the Debye length, and that high applied voltages and different pore shapes contribute to the different electric field enhancement and plasma properties. Models describing the influence of the nature of the catalyst on the plasma characteristics coupled with surface chemistry may play an essential role in designing, controlling and optimising plasma catalysis systems, and should be further developed and researched.

## 5. Conclusions and perspectives

As compared with conventional thermal activation, NTP activation of catalysts (in which plasma discharge dissociates reactant molecules in the gas phase and contributes to surface reactions, i.e. perturbation of the heterogeneous catalysis)

shows great potential in activating and converting stable  $\text{CO}_2$  molecules into value-added fuels and chemicals under comparatively mild conditions. Recent advances in plasma catalytic  $\text{CO}_2$  conversion (as discussed in this review), including  $\text{CO}$  splitting,  $\text{CO}_2$  hydrogenation into chemicals/fuels and reforming (with  $\text{CH}_4$  and  $\text{H}_2\text{O}$ ) into syngas, suggest that NTP-activated heterogeneous catalysis is a promising technology for the practical utilisation of  $\text{CO}_2$ .

Catalysts play an important role in hybrid systems regarding efficiency and selectivity. Thus, developing suitable catalysts specifically for NTP catalysis is critical to optimise hybrid systems for  $\text{CO}_2$  conversion, making it more competitive and economically attractive for practical applications. Previous studies have shown that the intrinsic properties of the catalysts, including the active metal species, metal particle size and the dispersion and location of active sites, and catalyst supports are the dominant factors in the performance of NTP catalysis. The development of bespoke NTP catalysts with highly dispersed metal active sites (e.g. single-atom catalysts) and hierarchical porous structures (e.g. modified MOFs and zeolite) are beneficial for maximising the plasma catalytic  $\text{CO}_2$  conversion processes. However, a fundamental understanding of the correlation on the structure–composition–activity is still needed to provide guidance on the rational design of cost-effective, highly selective and efficient catalysts specified for NTP catalysis.

Moreover, a comprehensive and in-depth understanding of plasma–catalyst interactions also is important in maximising NTP-assisted  $\text{CO}_2$  conversion. In the presence of a catalyst, an electric field can be enhanced due to the formation of surface discharge, benefiting  $\text{CO}_2$  activation and subsequent surface reactions. Compared with thermal catalysis, where heterogeneous catalysis proceeds only with the chemisorption of the reactant on the catalyst surface, plasma-induced reactive species in the gas phase may introduce new species for multiple surface reactions, thus lowering the reaction barriers and altering the reaction pathways of the catalysis. However, both chemical and physical effects are interlinked, and hence are difficult to be fully decoupled. Hence, hybrid plasma catalysis systems are highly complex and require further understanding to advance the technology. *In situ* techniques such as OES, XAFS and DRIFTS together with advanced modelling methods have shown the ability to gain relevant insights into NTP catalytic  $\text{CO}_2$  conversion. Further development and implementation of *in situ* characterisation techniques and relevant plasma modelling investigations on surface/gas-phase reactions, species transport, adsorption/desorption, reaction intermediate formation on active sites and the real-time change of catalyst surface in the hybrid NTP catalysis system are still needed to progress our understanding on the plasma–catalyst interactions and mechanisms of NTP catalysis.

Finally, the trade-off between energy efficiency and  $\text{CO}_2$  conversion still needs further investigation in plasma catalysis, especially for large-scale processes. It is important to develop reactor designs and optimise operating conditions to improve the energy efficiency of plasma catalytic  $\text{CO}_2$  conversion. For example, a water-cooled DBD reactor has been demonstrated to be more effective at producing liquid fuels

from CO<sub>2</sub> hydrogenation [52]. Also, novel integrated processes combining CO<sub>2</sub> capture [153] and the CO<sub>2</sub> separation process [154] with plasma catalytic CO<sub>2</sub> conversion have shown the feasibility and potential for developing a generic platform technology with improved CO<sub>2</sub> capture and utilisation efficiency. Additionally, the industrialisation of NTP catalysis systems should also consider economic aspects, such as the costs of catalysts, the energy supply and separation of products, and hence, thorough techno-economic and life cycle assessments are needed to develop practical CO<sub>2</sub> conversion applications from laboratory-developed plasma systems.

### Data availability statement

No new data were created or analysed in this study.

### Acknowledgments

S X acknowledges financial support of the Dean's Doctoral Scholar Awards from the University of Manchester. H C acknowledges financial support from the Jiangsu Specially-Appointed Professors Program and the National Natural Science Foundation of China (No. 22008109) and the Natural Science Foundation of Jiangsu Province (No. BK20200704). The UK Catalysis Hub is kindly thanked for resources and support provided via our membership of the UK Catalysis Hub Consortium and funded by EPSRC Grants: EP/R026939/1, EP/R026815/1, EP/R026645/1, EP/R027129/1 and EP/M013219/1 (biocatalysis).

### ORCID iD

Xiaolei Fan  <https://orcid.org/0000-0002-9039-6736>

### References

- [1] Roy S, Cherevotan A and Peter S C 2018 Thermochemical CO<sub>2</sub> hydrogenation to single carbon products: scientific and technological challenges *ACS Energy Lett.* **3** 1938–66
- [2] Goeppert A, Czaun M, Jones J P, Surya Prakash G K and Olah G A 2014 Recycling of carbon dioxide to methanol and derived products-closing the loop *Chem. Soc. Rev.* **43** 7995–8048
- [3] Ashford B and Tu X 2017 Non-thermal plasma technology for the conversion of CO<sub>2</sub> *Curr. Opin. Green Sustain. Chem.* **3** 45–49
- [4] Feng X, Liu H, He C, Shen Z and Wang T 2018 Synergistic effects and mechanism of a non-thermal plasma catalysis system in volatile organic compound removal: a review *Catal. Sci. Technol.* **8** 936–54
- [5] Gholami R, Stere C E, Goguet A and Hardacre C 2018 Non-thermal-plasma-activated de-NO<sub>x</sub> catalysis *Phil. Trans. R. Soc. A* **376** 20170054
- [6] Bogaerts A *et al* 2020 The 2020 plasma catalysis roadmap *J. Phys. D: Appl. Phys.* **53** 443001
- [7] Zeng Y and Tu X 2017 Plasma-catalytic hydrogenation of CO<sub>2</sub> for the cogeneration of CO and CH<sub>4</sub> in a dielectric barrier discharge reactor: effect of argon addition *J. Phys. D: Appl. Phys.* **50** 184004
- [8] Nizio M, Benrabbah R, Krzak M, Debek R, Motak M, Cavadias S, Gálvez M E and da Costa P 2016 Low temperature hybrid plasma-catalytic methanation over Ni–Ce–Zr hydrotalcite-derived catalysts *Catal. Commun.* **83** 14–17
- [9] Stere C E *et al* 2017 Non-thermal plasma activation of gold-based catalysts for low-temperature water–gas shift catalysis *Angew. Chem., Int. Ed. Engl.* **56** 5579–83
- [10] Xu S *et al* 2019 Sustaining metal–organic frameworks for water–gas shift catalysis by non-thermal plasma *Nat. Catal.* **2** 142–8
- [11] Tu X and Whitehead J C 2012 Plasma-catalytic dry reforming of methane in an atmospheric dielectric barrier discharge: understanding the synergistic effect at low temperature *Appl. Catal. B* **125** 439–48
- [12] Lee D H and Kim T 2013 Plasma–catalyst hybrid methanol-steam reforming for hydrogen production *Int. J. Hydrog. Energy* **38** 6039–43
- [13] Yap D, Tatibouët J-M and Batiot-Dupeyrat C 2018 Catalysis assisted by non-thermal plasma in dry reforming of methane at low temperature *Catal. Today* **299** 263–71
- [14] van Durme J, Dewulf J, Leys C and van Langenhove H 2008 Combining non-thermal plasma with heterogeneous catalysis in waste gas treatment: a review *Appl. Catal. B* **78** 324–33
- [15] Barboun P, Mehta P, Herrera F A, Go D B, Schneider W F and Hicks J C 2019 Distinguishing plasma contributions to catalyst performance in plasma-assisted ammonia synthesis *ACS Sustain. Chem. Eng.* **7** 8621–30
- [16] Peng P *et al* 2018 A review on the non-thermal plasma-assisted ammonia synthesis technologies *J. Clean. Prod.* **177** 597–609
- [17] Bogaerts A and Neyts E C 2018 Plasma technology: an emerging technology for energy storage *ACS Energy Lett.* **3** 1013–27
- [18] Liu M, Yi Y, Wang L, Guo H and Bogaerts A 2019 Hydrogenation of carbon dioxide to value-added chemicals by heterogeneous catalysis and plasma catalysis *Catalysts* **9** 275
- [19] Whitehead J C 2016 Plasma–catalysis: the known knowns, the known unknowns and the unknown unknowns *J. Phys. D: Appl. Phys.* **49** 243001
- [20] Neyts E C, Ostrikov K K, Sunkara M K and Bogaerts A 2015 Plasma catalysis: synergistic effects at the nanoscale *Chem. Rev.* **115** 13408–46
- [21] Mehta P, Barboun P, Go D B, Hicks J C and Schneider W F 2019 Catalysis enabled by plasma activation of strong chemical bonds: a review *ACS Energy Lett.* **4** 1115–33
- [22] Whitehead J C 2019 Plasma-catalysis: is it just a question of scale? *Front. Chem. Sci. Eng.* **13** 264–73
- [23] Kim J, Go D B and Hicks J C 2017 Synergistic effects of plasma–catalyst interactions for CH<sub>4</sub> activation *Phys. Chem. Chem. Phys.* **19** 13010–21
- [24] Neyts E C 2015 Plasma–surface interactions in plasma catalysis *Plasma Chem. Plasma Process.* **36** 185–212
- [25] Zhao T, Ullah N, Hui Y and Li Z 2019 Review of plasma-assisted reactions and potential applications for modification of metal–organic frameworks *Front. Chem. Sci. Eng.* **13** 444–57
- [26] Snoeckx R and Bogaerts A 2017 Plasma technology—a novel solution for CO<sub>2</sub> conversion? *Chem. Soc. Rev.* **46** 5805–63
- [27] Paulussen S, Verheyde B, Tu X, de Bie C, Martens T, Petrovic D, Bogaerts A and Sels B 2010 Conversion of carbon dioxide to value-added chemicals in atmospheric pressure dielectric barrier discharges *Plasma Sources Sci. Technol.* **19** 034015
- [28] Mei D, He Y-L, Liu S, Yan J and Tu X 2016 Optimization of CO<sub>2</sub> conversion in a cylindrical dielectric barrier discharge

- reactor using design of experiments *Plasma Process. Polym.* **13** 544–56
- [29] Bogaerts A, Kozak T, van Laer K and Snoeckx R 2015 Plasma-based conversion of CO<sub>2</sub>: current status and future challenges *Faraday Discuss.* **183** 217–32
- [30] Mei D and Tu X 2017 Conversion of CO<sub>2</sub> in a cylindrical dielectric barrier discharge reactor: effects of plasma processing parameters and reactor design *J. CO<sub>2</sub> Util.* **19** 68–78
- [31] Aerts R, Somers W and Bogaerts A 2015 Carbon dioxide splitting in a dielectric barrier discharge plasma: a combined experimental and computational study *ChemSusChem* **8** 702–16
- [32] Ramakers M, Michielsens I, Aerts R, Meynen V and Bogaerts A 2015 Effect of argon or helium on the CO<sub>2</sub> conversion in a dielectric barrier discharge *Plasma Process. Polym.* **12** 755–63
- [33] Lindon M A and Scime E E 2014 CO<sub>2</sub> dissociation using the versatile atmospheric dielectric barrier discharge experiment (VADER) *Front. Phys.* **2** 55
- [34] Mei D, Zhu X, He Y-L, Yan J D and Tu X 2014 Plasma-assisted conversion of CO<sub>2</sub> in a dielectric barrier discharge reactor: understanding the effect of packing materials *Plasma Sources Sci. Technol.* **24** 015011
- [35] Yu Q, Kong M, Liu T, Fei J and Zheng X 2011 Characteristics of the decomposition of CO<sub>2</sub> in a dielectric packed-bed plasma reactor *Plasma Process.* **32** 153–63
- [36] Michielsens I, Uytendhouwen Y, Pype J, Michielsens B, Mertens J, Reniers F, Meynen V and Bogaerts A 2017 CO<sub>2</sub> dissociation in a packed bed DBD reactor: first steps towards a better understanding of plasma catalysis *Chem. Eng. J.* **326** 477–88
- [37] Duan X, Hu Z, Li Y and Wang B 2015 Effect of dielectric packing materials on the decomposition of carbon dioxide using DBD microplasma reactor *AIChE J.* **61** 898–903
- [38] Xu S, Whitehead J C and Martin P A 2017 CO<sub>2</sub> conversion in a non-thermal, barium titanate packed bed plasma reactor: the effect of dilution by Ar and N<sub>2</sub> *Chem. Eng. J.* **327** 764–73
- [39] Butterworth T, Elder R and Allen R 2016 Effects of particle size on CO<sub>2</sub> reduction and discharge characteristics in a packed bed plasma reactor *Chem. Eng. J.* **293** 55–67
- [40] Zhou A, Chen D, Ma C, Yu F and Dai B 2018 DBD plasma-ZrO<sub>2</sub> catalytic decomposition of CO<sub>2</sub> at low temperatures *Catalysts* **8** 256
- [41] Mei D and Tu X 2017 Atmospheric pressure non-thermal plasma activation of CO<sub>2</sub> in a packed-bed dielectric barrier discharge reactor *ChemPhysChem* **18** 3253–9
- [42] Benrababah R, Cavaniol C, Liu H, Ognier S, Cavadias S, Gálvez M E and da Costa P 2017 Plasma DBD activated ceria-zirconia-promoted Ni-catalysts for plasma catalytic CO<sub>2</sub> hydrogenation at low temperature *Catal. Commun.* **89** 73–76
- [43] Zhu X, Liu J-H, Li X-S, Liu J-L, Qu X and Zhu A-M 2017 Enhanced effect of plasma on catalytic reduction of CO<sub>2</sub> to CO with hydrogen over Au/CeO<sub>2</sub> at low temperature *J. Energy Chem.* **26** 488–93
- [44] Jwa E, Lee S B, Lee H W and Mok Y S 2013 Plasma-assisted catalytic methanation of CO and CO<sub>2</sub> over Ni-zeolite catalysts *Fuel Process. Technol.* **108** 89–93
- [45] Biset-Peiró M, Guilera J, Zhang T, Arbiol J and Andreu T 2019 On the role of ceria in Ni-Al<sub>2</sub>O<sub>3</sub> catalyst for CO<sub>2</sub> plasma methanation *Appl. Catal. A* **575** 223–9
- [46] Lee C J, Lee D H and Kim T 2017 Enhancement of methanation of carbon dioxide using dielectric barrier discharge on a ruthenium catalyst at atmospheric conditions *Catal. Today* **293–294** 97–104
- [47] Ahmad F, Lovell E C, Masood H, Cullen P J, Ostrikov K K, Scott J A and Amal R 2020 Low-temperature CO<sub>2</sub> methanation: synergistic effects in plasma-Ni hybrid catalytic system *ACS Sustain. Chem. Eng.* **8** 1888–98
- [48] Mikhail M, Wang B, Jalain R, Cavadias S, Tatoulian M, Ognier S, Gálvez M E and da Costa P 2018 Plasma-catalytic hybrid process for CO<sub>2</sub> methanation: optimization of operation parameters *React. Kinet. Mech. Catal.* **126** 629–43
- [49] Alvarez A, Bansode A, Urakawa A, Bavykina A V, Wezendonk T A, Makkee M, Gascon J and Kapteijn F 2017 Challenges in the greener production of formates/formic acid, methanol, and DME by heterogeneously catalyzed CO<sub>2</sub> hydrogenation processes *Chem. Rev.* **117** 9804–38
- [50] Lan L, Wang A and Wang Y 2019 CO<sub>2</sub> hydrogenation to lower hydrocarbons over ZSM-5-supported catalysts in a dielectric-barrier discharge plasma reactor *Catal. Commun.* **130** 105761
- [51] Eliasson B, Kogelschatz U, Xue B and Zhou L-M 1998 Hydrogenation of carbon dioxide to methanol with a discharge-activated catalyst *Ind. Eng. Chem. Res.* **37** 3350–7
- [52] Wang L, Yi Y, Guo H and Tu X 2017 Atmospheric pressure and room temperature synthesis of methanol through plasma-catalytic hydrogenation of CO<sub>2</sub> *ACS Catal.* **8** 90–100
- [53] Men Y-L, Liu Y, Wang Q, Luo Z-H, Shao S, Li Y-B and Pan Y-X 2019 Highly dispersed Pt-based catalysts for selective CO<sub>2</sub> hydrogenation to methanol at atmospheric pressure *Chem. Eng. Sci.* **200** 167–75
- [54] Iliuta I and Larachi F 2019 Enhanced methanol synthesis process via an integrated process involving CO<sub>2</sub> hydrogenation under plasma conditions *Ind. Eng. Chem. Res.* **59** 6815–27
- [55] Chung W-C and Chang M-B 2016 Review of catalysis and plasma performance on dry reforming of CH<sub>4</sub> and possible synergistic effects *Renew. Sust. Energ. Rev.* **62** 13–31
- [56] Khoja A H, Tahir M and Amin N A S 2019 Recent developments in non-thermal catalytic DBD plasma reactor for dry reforming of methane *Energy Convers. Manage.* **183** 529–60
- [57] Puliyalil H, Lašič Jurković D, Dasireddy V D B C and Likozar B 2018 A review of plasma-assisted catalytic conversion of gaseous carbon dioxide and methane into value-added platform chemicals and fuels *RSC Adv.* **8** 27481–508
- [58] Ray D, Reddy P M K and Subrahmanyam C 2018 Ni-Mn/γ-Al<sub>2</sub>O<sub>3</sub> assisted plasma dry reforming of methane *Catal. Today* **309** 212–8
- [59] Khoja A H, Tahir M and Saidina Amin N A 2019 Evaluating the performance of a Ni catalyst supported on La<sub>2</sub>O<sub>3</sub>-MgAl<sub>2</sub>O<sub>4</sub> for dry reforming of methane in a packed bed dielectric barrier discharge plasma reactor *Energy Fuels* **33** 11630–47
- [60] Eliasson B, Liu C-J and Kogelschatz U 2000 Direct conversion of methane and carbon dioxide to higher hydrocarbons using catalytic dielectric-barrier discharges with zeolites *Ind. Eng. Chem. Res.* **39** 1221–7
- [61] Zeng Y, Zhu X, Mei D, Ashford B and Tu X 2015 Plasma-catalytic dry reforming of methane over γ-Al<sub>2</sub>O<sub>3</sub> supported metal catalysts *Catal. Today* **256** 80–7
- [62] Vakili R, Gholami R, Stere C E, Chansai S, Chen H, Holmes S M, Jiao Y, Hardacre C and Fan X 2020 Plasma-assisted catalytic dry reforming of methane (DRM) over metal-organic frameworks (MOFs)-based catalysts *Appl. Catal. B* **260** 118195
- [63] Wang L, Yi Y, Wu C, Guo H and Tu X 2017 One-step reforming of CO<sub>2</sub> and CH<sub>4</sub> into high-value liquid chemicals and fuels at room temperature by plasma-driven catalysis *Angew. Chem., Int. Ed. Engl.* **56** 13679–83

- [64] Snoeckx R, Ozkan A, Reniers F and Bogaerts A 2017 The quest for value-added products from carbon dioxide and water in a dielectric barrier discharge: a chemical kinetics study *ChemSusChem* **10** 409–24
- [65] Ma X, Li S, Ronda-Lloret M, Chaudhary R, Lin L, van Rooij G, Gallucci F, Rothenberg G, Raveendran Shiju N and Hessel V 2018 Plasma assisted catalytic conversion of CO<sub>2</sub> and H<sub>2</sub>O over Ni/Al<sub>2</sub>O<sub>3</sub> in a DBD reactor *Plasma Chem. Plasma Process.* **39** 109–24
- [66] Zhao B, Liu Y, Zhu Z, Guo H and Ma X 2018 Highly selective conversion of CO<sub>2</sub> into ethanol on Cu/ZnO/Al<sub>2</sub>O<sub>3</sub> catalyst with the assistance of plasma *J. CO<sub>2</sub> Util.* **24** 34–9
- [67] Ghaib K, Nitz K and Ben-Fares F Z 2016 Chemical methanation of CO<sub>2</sub>: a review *ChemBioEng Rev.* **3** 266–75
- [68] Younas M, Loong Kong L, Bashir M J K, Nadeem H, Shehzad A and Sethupathi S 2016 Recent advancements, fundamental challenges, and opportunities in catalytic methanation of CO<sub>2</sub> *Energy Fuels* **30** 8815–31
- [69] Ewald S, Kolbeck M, Kratky T, Wolf M and Hinrichsen O 2019 On the deactivation of Ni–Al catalysts in CO<sub>2</sub> methanation *Appl. Catal. A* **570** 376–86
- [70] Millet M-M, Tarasov A V, Girgsdies F, Algara-Siller G, Schlögl R and Frei E 2019 Highly dispersed Ni<sub>0</sub>/Ni<sub>x</sub>Mg<sub>1-x</sub>O catalysts derived from solid solutions: how metal and support control the CO<sub>2</sub> hydrogenation *ACS Catal.* **9** 8534–46
- [71] Guo Y, Mei S, Yuan K, Wang D-J, Liu H-C, Yan C-H and Zhang Y-W 2018 Low-temperature CO<sub>2</sub> methanation over CeO<sub>2</sub>-supported Ru single atoms, nanoclusters, and nanoparticles competitively tuned by strong metal–support interactions and H-spillover effect *ACS Catal.* **8** 6203–15
- [72] Kwak J H, Kovarik L and Szanyi J 2013 CO<sub>2</sub> reduction on supported Ru/Al<sub>2</sub>O<sub>3</sub> catalysts: cluster size dependence of product selectivity *ACS Catal.* **3** 2449–55
- [73] Yan Y, Wang Q, Jiang C, Yao Y, Lu D, Zheng J, Dai Y, Wang H and Yang Y 2018 Ru/Al<sub>2</sub>O<sub>3</sub> catalyzed CO<sub>2</sub> hydrogenation: oxygen-exchange on metal–support interfaces *J. Catal.* **367** 194–205
- [74] Chen C-S, Budi C S, Wu H-C, Saikia D and Kao H-M 2017 Size-tunable Ni nanoparticles supported on surface-modified, cage-type mesoporous silica as highly active catalysts for CO<sub>2</sub> hydrogenation *ACS Catal.* **7** 8367–81
- [75] Babucci M, Guntida A and Gates B C 2020 Atomically dispersed metals on well-defined supports including zeolites and metal–organic frameworks: structure, bonding, reactivity, and catalysis *Chem. Rev.* **120** 11956–85
- [76] Zhao Z-W, Zhou X, Liu Y-N, Shen C-C, Yuan C-Z, Jiang Y-F, Zhao S-J, Ma L-B, Cheang T-Y and Xu A-W 2018 Ultrasmall Ni nanoparticles embedded in Zr-based MOFs provide high selectivity for CO<sub>2</sub> hydrogenation to methane at low temperatures *Catal. Sci. Technol.* **8** 3160–5
- [77] Garbarino G, Bellotti D, Riani P, Magistri L and Busca G 2015 Methanation of carbon dioxide on Ru/Al<sub>2</sub>O<sub>3</sub> and Ni/Al<sub>2</sub>O<sub>3</sub> catalysts at atmospheric pressure: catalysts activation, behaviour and stability *Int. J. Hydrog. Energy* **40** 9171–82
- [78] Mutschler R, Moioli E, Luo W, Gallandat N and Züttel A 2018 CO<sub>2</sub> hydrogenation reaction over pristine Fe, Co, Ni, Cu and Al<sub>2</sub>O<sub>3</sub> supported Ru: comparison and determination of the activation energies *J. Catal.* **366** 139–49
- [79] Garbarino G, Riani P, Magistri L and Busca G 2014 A study of the methanation of carbon dioxide on Ni/Al<sub>2</sub>O<sub>3</sub> catalysts at atmospheric pressure *Int. J. Hydrog. Energy* **39** 11557–65
- [80] Ye R-P *et al* 2019 Enhanced stability of Ni/SiO<sub>2</sub> catalyst for CO<sub>2</sub> methanation: derived from nickel phyllosilicate with strong metal–support interactions *Energy* **188** 116059
- [81] Kim A, Debecker D P, Devred F, Dubois V, Sanchez C and Sassoie C 2018 CO<sub>2</sub> methanation on Ru/TiO<sub>2</sub> catalysts: on the effect of mixing anatase and rutile TiO<sub>2</sub> supports *Appl. Catal. B* **220** 615–25
- [82] Lin J, Ma C, Wang Q, Xu Y, Ma G, Wang J, Wang H, Dong C, Zhang C and Ding M 2019 Enhanced low-temperature performance of CO<sub>2</sub> methanation over mesoporous Ni/Al<sub>2</sub>O<sub>3</sub>–ZrO<sub>2</sub> catalysts *Appl. Catal. B* **243** 262–72
- [83] Winter L R, Gomez E, Yan B, Yao S and Chen J G 2018 Tuning Ni-catalyzed CO<sub>2</sub> hydrogenation selectivity via Ni–ceria support interactions and Ni–Fe bimetallic formation *Appl. Catal. B* **224** 442–50
- [84] Graça I, González L V, Bacariza M C, Fernandes A, Henriques C, Lopes J M and Ribeiro M F 2014 CO<sub>2</sub> hydrogenation into CH<sub>4</sub> on NiHNaUSY zeolites *Appl. Catal. B* **147** 101–10
- [85] Le T A, Kim M S, Lee S H, Kim T W and Park E D 2017 CO and CO<sub>2</sub> methanation over supported Ni catalysts *Catal. Today* **293–294** 89–96
- [86] Zhou G, Liu H, Cui K, Jia A, Hu G, Jiao Z, Liu Y and Zhang X 2016 Role of surface Ni and Ce species of Ni/CeO<sub>2</sub> catalyst in CO<sub>2</sub> methanation *Appl. Surf. Sci.* **383** 248–52
- [87] Italiano C, Llorca J, Pino L, Ferraro M, Antonucci V and Vita A 2020 CO and CO<sub>2</sub> methanation over Ni catalysts supported on CeO<sub>2</sub>, Al<sub>2</sub>O<sub>3</sub> and Y<sub>2</sub>O<sub>3</sub> oxides *Appl. Catal. B* **264** 118494
- [88] Wang F, He S, Chen H, Wang B, Zheng L, Wei M, Evans D G and Duan X 2016 Active site dependent reaction mechanism over Ru/CeO<sub>2</sub> catalyst toward CO<sub>2</sub> methanation *J. Am. Chem. Soc.* **138** 6298–305
- [89] Cárdenas-Arenas A, Quindimil A, Davó-Quiñero A, Bailón-García E, Lozano-Castelló D, De-La-Torre U, Pereda-Ayo B, González-Marcos J A, González-Velasco J R and Bueno-López A 2020 Isotopic and *in situ* DRIFTS study of the CO<sub>2</sub> methanation mechanism using Ni/CeO<sub>2</sub> and Ni/Al<sub>2</sub>O<sub>3</sub> catalysts *Appl. Catal. B* **265** 118538
- [90] Ye R-P *et al* 2020 High-performance of nanostructured Ni/CeO<sub>2</sub> catalyst on CO<sub>2</sub> methanation *Appl. Catal. B* **268** 118474
- [91] Lee W J, Li C, Prajitno H, Yoo J, Patel J, Yang Y and Lim S 2020 Recent trend in thermal catalytic low temperature CO<sub>2</sub> methanation: a critical review *Catal. Today* (<https://doi.org/10.1016/j.cattod.2020.02.017>)
- [92] Zeng Y and Tu X 2016 Plasma-catalytic CO<sub>2</sub> hydrogenation at low temperatures *IEEE Trans. Plasma Sci.* **44** 405–11
- [93] Oshima K, Shinagawa T, Nogami Y, Manabe R, Ogo S and Sekine Y 2014 Low temperature catalytic reverse water gas shift reaction assisted by an electric field *Catal. Today* **232** 27–32
- [94] Sun Y, Li J, Chen P, Wang B, Wu J and Fu M, Chen L and Ye D 2020 Reverse water–gas shift in a packed bed DBD reactor: investigation of metal–support interface towards a better understanding of plasma catalysis *Appl. Catal. A* **591** 117407
- [95] Liu L, Zhang Z, Das S, Xi S and Kawi S 2020 LaNiO<sub>3</sub> as a precursor of Ni/La<sub>2</sub>O<sub>3</sub> for reverse water–gas shift in DBD plasma: effect of calcination temperature *Energy Convers. Manage.* **206** 112475
- [96] Xu W, Zhang X, Dong M, Zhao J and Di L 2019 Plasma-assisted Ru/Zr-MOF catalyst for hydrogenation of CO<sub>2</sub> to methane *Plasma Sci. Technol.* **21** 044004
- [97] Xu W, Dong M, Di L and Zhang X 2019 A facile method for preparing UiO-66 encapsulated Ru catalyst and its

- application in plasma-assisted CO<sub>2</sub> methanation *Nanomaterials* **9** 1432
- [98] Wierzbicki D, Moreno M V, Ognier S, Motak M, Grzybek T, da Costa P and Gálvez M E 2020 Ni–Fe layered double hydroxide derived catalysts for non-plasma and DBD plasma-assisted CO<sub>2</sub> methanation *Int. J. Hydrog. Energy* **45** 10423–32
- [99] Wang Z, Zhang Y, Neyts E C, Cao X, Zhang X, Jang B W L and Liu C-J 2018 Catalyst preparation with plasmas: how does it work? *ACS Catal.* **8** 2093–110
- [100] Chawdhury P, Bhargavi K V S S, Selvaraj M and Subrahmanyam C 2020 Promising catalytic activity by non-thermal plasma synthesized SBA-15-supported metal catalysts in one-step plasma-catalytic methane conversion to value-added fuels *Catal. Sci. Technol.* **10** 5566
- [101] Nizio M, Albarazi A, Cavadias S, Amouroux J, Galvez M E and da Costa P 2016 Hybrid plasma-catalytic methanation of CO<sub>2</sub> at low temperature over ceria zirconia supported Ni catalysts *Int. J. Hydrog. Energy* **41** 11584–92
- [102] Mok Y S, Jwa E and Lee H W 2013 Production of methane from carbon monoxide and carbon dioxide in a plasma-catalytic combined reactor system *Int. J. Sustain. Dev. Plan.* **8** 186–96
- [103] Chen H, Mu Y, Shao Y, Chansai S, Xiang H, Jiao Y, Hardacre C and Fan X 2019 Nonthermal plasma (NTP) activated metal–organic frameworks (MOFs) catalyst for catalytic CO<sub>2</sub> hydrogenation *AIChE J.* **66** 16853
- [104] Amouroux J and Cavadias S 2017 Electrocatalytic reduction of carbon dioxide under plasma DBD process *J. Phys. D: Appl. Phys.* **50** 465501
- [105] Chen H *et al* 2019 Coupling non-thermal plasma with Ni catalysts supported on BETA zeolite for catalytic CO<sub>2</sub> methanation *Catal. Sci. Technol.* **9** 4135–45
- [106] Bacariza M C, Biset-Peiró M, Graça I, Guilera J, Morante J, Lopes J M, Andreu T and Henriques C 2018 DBD plasma-assisted CO<sub>2</sub> methanation using zeolite-based catalysts: structure composition-reactivity approach and effect of Ce as promoter *J. CO<sub>2</sub> Util.* **26** 202–11
- [107] Mei D, Ashford B, He Y-L and Tu X 2017 Plasma-catalytic reforming of biogas over supported Ni catalysts in a dielectric barrier discharge reactor: effect of catalyst supports *Plasma Process. Polym.* **14** 1600076
- [108] Li P, Yu F, Altaf N, Zhu M, Li J, Dai B and Wang Q 2018 Two-dimensional layered double hydroxides for reactions of methanation and methane reforming in C1 chemistry *Materials* **11** 221
- [109] Dewangan N, Hui W M, Jayaprakash S, Bawah A-R, Poerjoto A J, Jie T, Jangam A, Hidajat K and Kawi S 2020 Recent progress on layered double hydroxide (LDH) derived metal-based catalysts for CO<sub>2</sub> conversion to valuable chemicals *Catal. Today* **356** 490–513
- [110] Xu S *et al* 2020 Mechanistic study of non-thermal plasma assisted CO<sub>2</sub> hydrogenation over Ru supported on MgAl layered double hydroxide *Appl. Catal. B* **268** 118752
- [111] Masoumifard N, Guillet-Nicolas R and Kleitz F 2018 Synthesis of engineered zeolitic materials: from classical zeolites to hierarchical core–shell materials *Adv. Mater.* **30** 1704439
- [112] Zhang Q, Yu J and Corma A 2020 Applications of zeolites to C1 chemistry: recent advances, challenges, and opportunities *Adv. Mater.* **32** 2002927
- [113] Zhang Y-R, Neyts E C and Bogaerts A 2018 Enhancement of plasma generation in catalyst pores with different shapes *Plasma Sources Sci. Technol.* **27** 055008
- [114] Zhang Y-R, van Laer K, Neyts E C and Bogaerts A 2016 Can plasma be formed in catalyst pores? A modeling investigation *Appl. Catal. B* **185** 56–67
- [115] Bogaerts A, Zhang Q-Z, Zhang Y-R, van Laer K and Wang W 2019 Burning questions of plasma catalysis: answers by modeling *Catal. Today* **337** 3–14
- [116] Zhang Y, Wang H-Y, Zhang Y-R and Bogaerts A 2017 Formation of microdischarges inside a mesoporous catalyst in dielectric barrier discharge plasmas *Plasma Sources Sci. Technol.* **26** 054002
- [117] Thevenet F, Sivachandiran L, Guaitella O, Barakat C and Rousseau A 2014 Plasma–catalyst coupling for volatile organic compound removal and indoor air treatment: a review *J. Phys. D: Appl. Phys.* **47** 224011
- [118] Chen H, Lee H, Chen S, Chao Y and Chang M 2008 Review of plasma catalysis on hydrocarbon reforming for hydrogen production—interaction, integration, and prospects *Appl. Catal. B* **85** 1–9
- [119] Chen H, Goodarzi F, Mu Y, Chansai S, Mielby J J, Mao B, Sooknoi T, Hardacre C, Kegnaes S and Fan X 2020 Effect of metal dispersion and support structure of Ni/silicalite-1 catalysts on non-thermal plasma (NTP) activated CO<sub>2</sub> hydrogenation *Appl. Catal. B* **272** 119013
- [120] Huang Y-B, Liang J, Wang X-S and Cao R 2017 Multifunctional metal–organic framework catalysts: synergistic catalysis and tandem reactions *Chem. Soc. Rev.* **46** 126–57
- [121] Maina J W, Pozo-Gonzalo C, Kong L, Schütz J, Hill M and Dumée L F 2017 Metal organic framework based catalysts for CO<sub>2</sub> conversion *Mater. Horiz.* **4** 345–61
- [122] Bacariza M C, Bértolo R, Graça I, Lopes J M and Henriques C 2017 The effect of the compensating cation on the catalytic performances of Ni/USY zeolites towards CO<sub>2</sub> methanation *J. CO<sub>2</sub> Util.* **21** 280–91
- [123] Petala A and Panagiotopoulou P 2018 Methanation of CO<sub>2</sub> over alkali-promoted Ru/TiO<sub>2</sub> catalysts: I. Effect of alkali additives on catalytic activity and selectivity *Appl. Catal. B* **224** 919–27
- [124] Liang B, Duan H, Sun T, Ma J, Liu X, Xu J, Su X, Huang Y and Zhang T 2018 Effect of Na promoter on Fe-based catalyst for CO<sub>2</sub> hydrogenation to alkenes *ACS Sustain. Chem. Eng.* **7** 925–32
- [125] Ray D, Chawdhury P and Subrahmanyam C 2020 Promising utilization of CO<sub>2</sub> for syngas production over Mg<sup>2+</sup>- and Ce<sup>2+</sup>-promoted Ni/gamma-Al<sub>2</sub>O<sub>3</sub> assisted by nonthermal plasma *ACS Omega* **5** 14040–50
- [126] Bacariza M C, Graça I, Bebiano S S, Lopes J M and Henriques C 2017 Magnesium as promoter of CO<sub>2</sub> methanation on Ni-based USY zeolites *Energy Fuels* **31** 9776–89
- [127] Wang H, Zhao B, Qin L, Wang Y, Yu F and Han J 2020 Non-thermal plasma-enhanced dry reforming of methane and CO<sub>2</sub> over Ce-promoted Ni/C catalysts *Mol. Catal.* **485** 110821
- [128] Zeng Y X, Wang L, Wu C F, Wang J Q, Shen B X and Tu X 2018 Low temperature reforming of biogas over K-, Mg- and Ce-promoted Ni/Al<sub>2</sub>O<sub>3</sub> catalysts for the production of hydrogen rich syngas: understanding the plasma-catalytic synergy *Appl. Catal. B* **224** 469–78
- [129] Khoja A H, Tahir M and Amin N A S 2018 Cold plasma dielectric barrier discharge reactor for dry reforming of methane over Ni/γ-Al<sub>2</sub>O<sub>3</sub>–MgO nanocomposite *Fuel Process. Technol.* **178** 166–79
- [130] Neyts E and Bogaerts A 2014 Understanding plasma catalysis through modelling and simulation—a review *J. Phys. D: Appl. Phys.* **47** 224010
- [131] Smith R, Killelea D, DelSesto D and Utz A 2004 Preference for vibrational over translational energy in a gas–surface reaction *Science* **304** 992–5
- [132] Jafarzadeh A, Bal K, Bogaerts A and Neyts E 2019 CO<sub>2</sub> activation on TiO<sub>2</sub>-supported Cu<sub>5</sub> and Ni<sub>5</sub> nanoclusters:

- effect of plasma-induced surface charging *J. Phys. Chem. C* **123** 6516–25
- [133] Lee B-Y, Park S-H, Lee S-C, Kang M and Choung S-J 2004 Decomposition of benzene by using a discharge plasma–photocatalyst hybrid system *Catal. Today* **93–95** 769–76
- [134] Guaitella O, Thevenet F, Puzenat E, Guillard C and Rousseau A 2008 C<sub>2</sub>H<sub>2</sub> oxidation by plasma/TiO<sub>2</sub> combination: influence of the porosity, and photocatalytic mechanisms under plasma exposure *Appl. Catal. B* **80** 296–305
- [135] Kim H-H and Ogata A 2011 Nonthermal plasma activates catalyst: from current understanding and future prospects *Eur. Phys. J. Appl. Phys.* **55** 13806
- [136] Chen H, Mu Y, Xu S, Xu S, Hardacre C and Fan X 2020 Recent advances in non-thermal plasma (NTP) catalysis towards C1 chemistry *Chin. J. Chem. Eng.* **28** 2010–21
- [137] Mu Y, Xu S, Shao Y, Chen H, Hardacre C and Fan X 2020 Kinetic study of nonthermal plasma activated catalytic CO<sub>2</sub> hydrogenation over Ni supported on silica catalyst *Ind. Eng. Chem. Res.* **59** 9478–87
- [138] Parastaev A, Hoeben W F L M, van Heesch B E J M, Kosinov N and Hensen E J M 2018 Temperature-programmed plasma surface reaction: an approach to determine plasma-catalytic performance *Appl. Catal. B* **239** 168–77
- [139] Azzolina-Jury F and Thibault-Starzyk F 2017 Mechanism of low pressure plasma-assisted CO<sub>2</sub> hydrogenation over Ni–USY by microsecond time-resolved FTIR spectroscopy *Top. Catal.* **60** 1709–21
- [140] Stere C, Chansai S, Gholami R, Wangkawong K, Singhania A, Goguet A, Inceesungvorn B and Hardacre C 2020 A design of a fixed bed plasma DRIFTS cell for studying the NTP-assisted heterogeneously catalysed reactions *Catal. Sci. Technol.* **10** 1458–66
- [141] Stere C E, Adress W, Burch R, Chansai S, Goguet A, Graham W G and Hardacre C 2015 Probing a non-thermal plasma activated heterogeneously catalyzed reaction using *in situ* DRIFTS-MS *ACS Catal.* **5** 956–64
- [142] Stere C E, Adress W, Burch R, Chansai S, Goguet A, Graham W G, de Rosa F, Palma V and Hardacre C 2014 Ambient temperature hydrocarbon selective catalytic reduction of NO<sub>x</sub> using atmospheric pressure nonthermal plasma activation of a Ag/Al<sub>2</sub>O<sub>3</sub> catalyst *ACS Catal.* **4** 666–73
- [143] Azzolina-Jury F, Bento D, Henriques C and Thibault-Starzyk F 2017 Chemical engineering aspects of plasma-assisted CO<sub>2</sub> hydrogenation over nickel zeolites under partial vacuum *J. CO<sub>2</sub> Util.* **22** 97–109
- [144] Sheng Z, Kim H H, Yao S and Nozaki T 2020 Plasma-chemical promotion of catalysis for CH<sub>4</sub> dry reforming: unveiling plasma-enabled reaction mechanisms *Phys. Chem. Chem. Phys.* **22** 19349–58
- [145] Gibson E K *et al* 2017 Probing the role of a non-thermal plasma (NTP) in the hybrid NTP catalytic oxidation of methane *Angew. Chem., Int. Ed. Engl.* **56** 9351–5
- [146] Bersani M, Gupta K, Mishra A K, Lanza R, Taylor S F R, Islam H-U, Hollingsworth N, Hardacre C, de Leeuw N H and Darr J A 2016 Combined EXAFS, XRD, DRIFTS, and DFT study of nano copper-based catalysts for CO<sub>2</sub> hydrogenation *ACS Catal.* **6** 5823–33
- [147] Tsoukalou A, Abdala P M, Stoian D, Huang X, Willinger M G, Fedorov A and Muller C R 2019 Structural evolution and dynamics of an In<sub>2</sub>O<sub>3</sub> catalyst for CO<sub>2</sub> hydrogenation to methanol: an operando XAS-XRD and *in situ* TEM study *J. Am. Chem. Soc.* **141** 13497–505
- [148] Giorgianni G *et al* 2020 Elucidating the mechanism of the CO<sub>2</sub> methanation reaction over Ni–Fe hydrotalcite-derived catalysts via surface-sensitive *in situ* XPS and NEXAFS *Phys. Chem. Chem. Phys.* **22** 18788–97
- [149] Bogaerts A, de Bie C, Snoeckx R and Kozák T 2017 Plasma based CO<sub>2</sub> and CH<sub>4</sub> conversion: a modeling perspective *Plasma Process. Polym.* **14** 1600070
- [150] de Bie C, van Dijk J and Bogaerts A 2016 CO<sub>2</sub> hydrogenation in a dielectric barrier discharge plasma revealed *J. Phys. Chem. C* **120** 25210–24
- [151] Heijkens S, Aghaei M and Bogaerts A 2020 Plasma-based CH<sub>4</sub> conversion into higher hydrocarbons and H<sub>2</sub>: modeling to reveal the reaction mechanisms of different plasma sources *J. Phys. Chem. C* **124** 7016–30
- [152] de Bie C, van Dijk J and Bogaerts A 2015 The dominant pathways for the conversion of methane into oxygenates and syngas in an atmospheric pressure dielectric barrier discharge *J. Phys. Chem. C* **119** 22331–50
- [153] Moss M, Reed D G, Allen R W K and Styring P 2017 Integrated CO<sub>2</sub> capture and utilization using non-thermal plasmolysis *Front. Energy Res.* **5** 1–11
- [154] Chen H, Mu Y, Hardacre C and Fan X 2020 Integration of membrane separation with nonthermal plasma catalysis: a proof-of-concept for CO<sub>2</sub> capture and utilization *Ind. Eng. Chem. Res.* **59** 8202–11